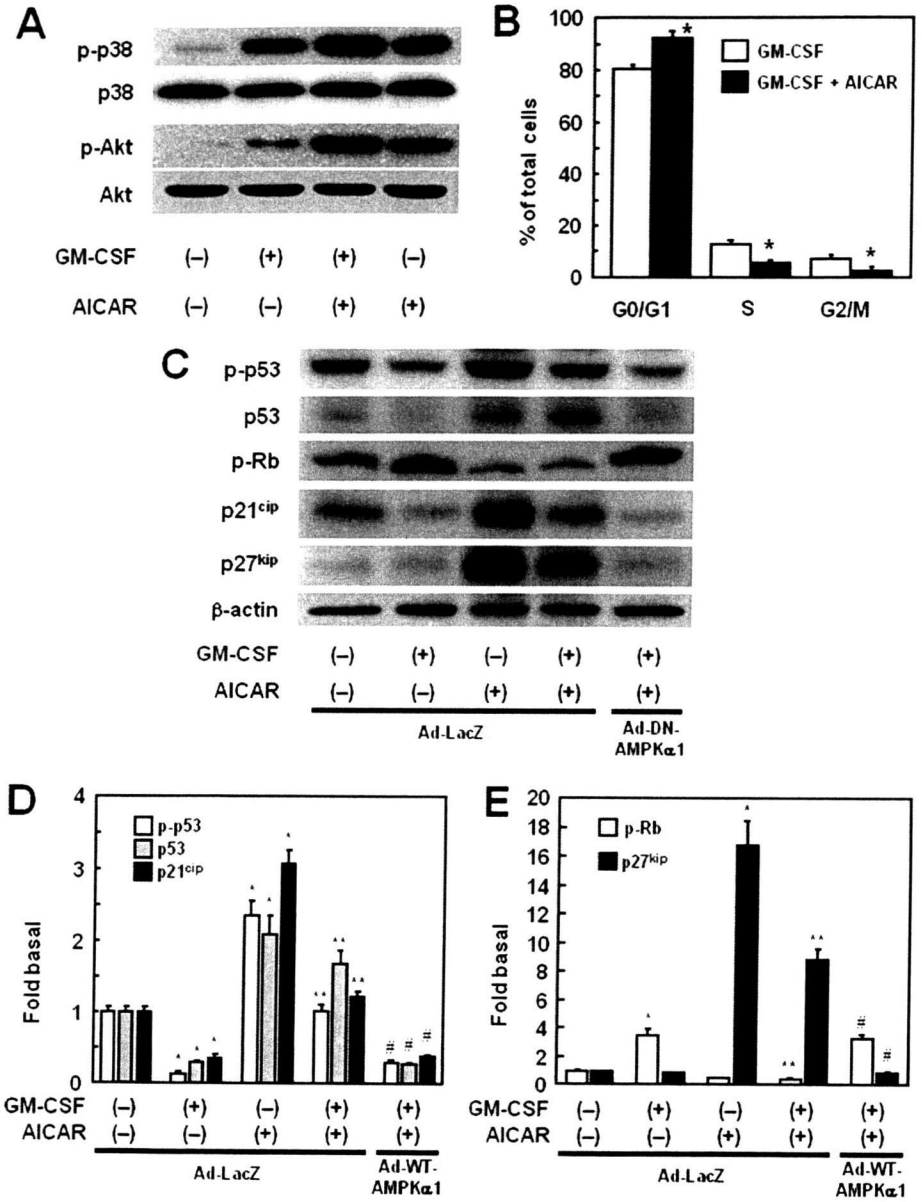

FIGURE 6. **AICAR induces cell cycle arrest.** *A–C*, macrophages were left untreated (*A* and *B*) or infected with adenoviral vectors containing LacZ (Ad-LacZ) and dominant-negative AMPKα1 (Ad-DN-AMPKα1) (*C*) and then cultured for 48 h. After treatment with 100 μM AICAR for 1 h, the cells were cultured with 10 pM GM-CSF for 30 min (*A*), 24 h (*C*), or 4 days (*B*). *A*, *C*, *D*, and *E*, protein samples were immunoblotted with anti-phospho-p38 MAPK (*p-p38*), anti-p38 MAPK (*p-p38*), anti-phospho-Akt (*p-Akt*), anti-Akt, anti-phospho-p53 (*p-p53*), anti-p53, anti-phospho-Rb (*p-Rb*), anti-p21^{cip}, anti-p27^{kip}, or anti-β-actin antibodies. Data represent the means ± S.E. of four separate experiments. Quantitative results for phosphorylated p53, total p53, and p21^{cip} (*D*), and phosphorylated Rb and p27^{kip} (E) were normalized by the levels of β-actin. *B*, the cell cycle distribution was determined by flow cytometry. Data represent the means ± S.E. of five separate experiments. *, $p < 0.01$, compared with untreated cells infected with Ad-LacZ. **, $p < 0.01$, compared with Ad-LacZ-infected cells incubated with GM-CSF alone. #, $p < 0.01$, compared with Ad-LacZ-infected cells incubated with GM-CSF and AICAR.

mechanisms other than apoptosis are involved in the suppression of macrophage proliferation.

Our previous studies indicated that Ox-LDL-induced GM-CSF production is mainly involved in macrophage proliferation (8, 11). Therefore, the mechanisms of Ox-LDL-induced macrophage proliferation can be divided into two parts: (i) intracellular signaling pathway before GM-CSF release, and (ii) proliferation signaling pathway through GM-CSF receptors. We demonstrated previously that Ox-LDL induces ERK1/2 activation and subsequently leads to GM-CSF expression in macrophages (8, 11). Hence, ERK1/2-dependent GM-CSF expression is one of the key phenomena for Ox-LDL-induced macrophage proliferation. AMPK activation suppresses angiotensin II-induced ERK1/2 activation in SMCs (22). On the other hand, AMPK activation does not suppress lipopolysaccharide-induced ERK1/2 activation in RAW264.7 cells (23). Therefore, the effects of AMPK activation on ERK1/2 activation may depend on the cell types involved or its inducers. In the present study, we found that AMPK activation suppressed Ox-LDL-induced ERK1/2 activation by 22% and GM-CSF protein and mRNA expressions by 29 and 25%, respectively, in mouse peritoneal macrophages. These results suggest that suppression of the GM-CSF expression pathway is only partially involved and that other mechanisms, such as modification of the downstream signaling pathway of GM-CSF release, are involved in AMPK-mediated suppression of macrophage proliferation.

As expected, we found that AMPK activation suppressed the macrophage proliferation induced by GM-CSF, suggesting that AMPK activation inhibits Ox-LDL-induced macrophage proliferation by suppressing the subsequent signaling of GM-CSF release. We further found that AMPK activation did not suppress p38 MAPK/Akt signaling, which is involved in GM-CSF-induced macrophage proliferation. Therefore, we speculated that the suppressive effects of AMPK on Ox-LDL-induced macrophage proliferation depended on cell cycle arrest, and subsequently found that AICAR significantly increased the percentage of cells in G_0/G_1 phase and decreased the percentages in S phase and G_2/M phase. Therefore, AMPK-induced cell cycle arrest should be the main cause of the AMPK-mediated suppression of macrophage proliferation.

Mammalian cell proliferation is controlled by the cell cycle machinery. Cell cycle progression is managed positively by CDKs and their cyclin-regulatory subunits (34) and managed negatively by CDKIs and tumor suppressor genes (35). Mito-

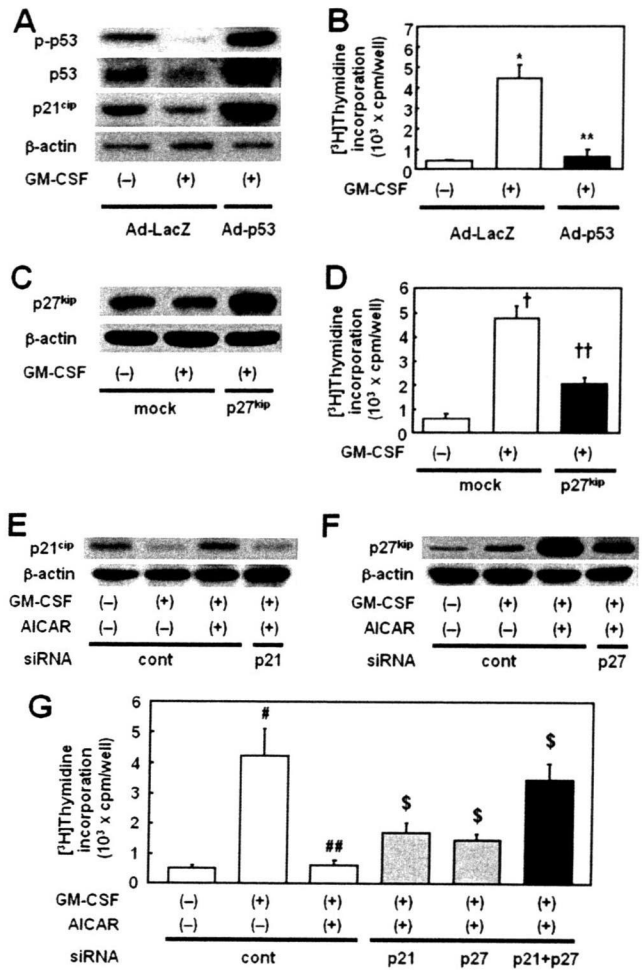

FIGURE 7. **AICAR-induced expression of $p21^{cip}$ and $p27^{kip}$ is involved in AICAR-mediated suppression of macrophage proliferation.** Macrophages were infected with adenoviral vectors containing LacZ (Ad-LacZ) or wild-type p53 (Ad-p53) (*A* and *B*), transfected with empty plasmid (*mock*) or plasmid containing $p27^{kip}$ (*C* and *D*), or transfected with siRNA for control (*cont*), $p21^{cip}$ (*p21*) or $p27^{kip}$ (*p27*) (*E–G*), and the cells were incubated for 24 h (*C–G*) or 48 h (*A* and *B*) Then the cells were treated with 10 pM GM-CSF in the absence or presence of 100 μM AICAR for 24 h (*A, C, E,* and *F*) or 5 days (*B, D,* and *G*). *A, C, E,* and *F*, protein samples were immunoblotted with anti-phospho-p53 (p-p53), anti-p53, anti-$p21^{cip}$, anti-$p27^{kip}$, or anti-β-actin antibodies. *B, D,* and *G*, [^{3}H]thymidine incorporation assays were performed. Data represent the means ± S.E. of four separate experiments. *, $p < 0.01$, compared with untreated cells infected with Ad-LacZ. **, $p < 0.01$, compared with Ad-LacZ-infected cells incubated with GM-CSF alone. †, $p < 0.01$, compared with untreated cells transfected with mock. ††, $p < 0.01$, compared with transected with mock and incubated with GM-CSF alone. #, $p < 0.01$, compared with untreated cells transfected with control siRNA. ##, $p < 0.01$, compared with cells transfected with control siRNA and incubated with GM-CSF alone. $, $p < 0.01$, compared with cells transfected with control siRNA and incubated with GM-CSF plus AICAR.

genic factors bind to their receptors and initiate a series of events resulting in the activation of CDKs, which in turn regulate cell cycle progression, DNA synthesis, DNA replication, and mitosis. The final common pathway leading to the $G_0/G_1/S$ transition is the CDK-induced hyperphosphorylation of Rb, which functions as a molecular switch that commits a cell to DNA replication. We found that GM-CSF phosphorylated Rb protein in macrophages and that this effect was suppressed by AICAR. Therefore, AMPK activation induces cell cycle arrest via inactivation of Rb.

CDKIs, such as $p21^{cip}$ and $p27^{kip}$, negatively regulate the cell cycle by inhibiting cyclin/CDK activities and Rb phosphorylation, resulting in G_1 arrest (36). On the other hand, the expression and functions of the tumor suppressor p53 are tightly regulated by its phosphorylation state. Cellular stresses, such as γ-irradiation and glucose deprivation, induce phosphorylation of p53 at Ser-15 (37, 33). The phosphorylated p53 induces cell-growth arrest and/or apoptosis through transcriptional regulation of p53 response genes such as $p21^{cip}$ and p53AIP1 (39). It has been reported that AMPK activation by AICAR inhibits the proliferation of various cancer cell lines *in vitro* and *in vivo* by increasing $p21^{cip}$, $p27^{kip}$, and p53 (38). Our group previously reported that AMPK activation suppresses the proliferation of vascular SMCs by increasing the phosphorylation of p53 and subsequent expression of $p21^{cip}$ (21). In macrophages, we newly found that GM-CSF suppressed the phosphorylation of p53 and expression of $p21^{cip}$ and that AICAR restored these effects. Interestingly, expression of $p27^{kip}$ was not abundant in unstimulated macrophages and remained unaffected by GM-CSF. However, AICAR drastically increased the expression of $p27^{kip}$. Moreover, we found that AICAR alone increased the phosphorylation and expression of p53 and the expression of $p21^{cip}$ and $p27^{kip}$. Furthermore, the overexpression of p53-$p21^{cip}$ and $p27^{kip}$ suppressed GM-CSF-induced macrophage proliferation, and the knockdown of $p21^{cip}$ and $p27^{kip}$ attenuated AICAR-mediated suppression of macrophage proliferation. These results suggest that the suppressive effects of AMPK activation on macrophage proliferation were mediated not by the interruption of GM-CSF-mediated intracellular signal pathway but by direct cell cycle arrest through the induction of p53 phosphorylation, $p21^{cip}$ expression, and $p27^{kip}$ expression.

In conclusion, we have revealed for the first time that activation of AMPK suppresses Ox-LDL-induced macrophage proliferation by inhibiting the expression of GM-CSF and inducing cell cycle arrest. Because the proliferation of vascular cells including macrophages is a key event in the development and progression of atherosclerosis (1, 3–5), the suppressive effect of AMPK activation on cell proliferation may be a therapeutic target for atherosclerosis.

Acknowledgments—We greatly appreciate the technical assistance from members of the Gene Technology Center (Kumamoto University), as well as Kenshi Ichinose.

REFERENCES

1. Ross, R. (1999) *N. Engl. J. Med.* **340,** 115–126
2. Steinberg, D., Parthasarathy, S., Carew, T. E., Khoo, J. C., and Witztum, J. L. (1989) *N. Engl. J. Med.* **320,** 915–924
3. Gordon, D., Reidy, M. A., Benditt, E. P., and Schwartz, S. M. (1990) *Proc. Natl. Acad. Sci. U.S.A.* **87,** 4600–4604
4. Rosenfeld, M. E., and Ross, R. (1990) *Arteriosclerosis* **10,** 680–687
5. Spagnoli, L. G., Orlandi, A., and Santeusanio, G. (1991) *Atherosclerosis* **88,** 87–92
6. Sakai, M., Miyazaki, A., Hakamata, H., Sasaki, T., Yui, S., Yamazaki, M., Shichiri, M., and Horiuchi, S. (1994) *J. Biol. Chem.* **269,** 31430–31435
7. Matsumura, T., Sakai, M., Kobori, S., Biwa, T., Takemura, T., Matsuda, H., Hakamata, H., Horiuchi, S., and Shichiri, M. (1997) *Arterioscler. Thromb. Vasc. Biol.* **17,** 3013–3020
8. Senokuchi, T., Matsumura, T., Sakai, M., Matsuo, T., Yano, M., Kiritoshi,

S., Sonoda, K., Kukidome, D., Nishikawa, T., and Araki, E. (2004) *Atherosclerosis* **176,** 233–245
9. Martens, J. S., Reiner, N. E., Herrera-Velit, P., and Steinbrecher, U. P. (1998) *J. Biol. Chem.* **273,** 4915–4920
10. Hamilton, J. A., Myers, D., Jessup, W., Cochrane, F., Byrne, R., Whitty, G., and Moss, S. (1999) *Arterioscler. Thromb. Vasc. Biol.* **19,** 98–105
11. Biwa, T., Hakamata, H., Sakai, M., Miyazaki, A., Suzuki, H., Kodama, T., Shichiri, M., and Horiuchi, S. (1998) *J. Biol. Chem.* **273,** 28305–28313
12. Matsumura, T., Sakai, M., Matsuda, K., Furukawa, N., Kaneko, K., and Shichiri, M. (1999) *J. Biol. Chem.* **274,** 37665–37672
13. Biwa, T., Sakai, M., Matsumura, T., Kobori, S., Kaneko, K., Miyazaki, A., Hakamata, H., Horiuchi, S., and Shichiri, M. (2000) *J. Biol. Chem.* **275,** 5810–5816
14. Hardie, D. G., Carling, D., and Carlson, M. (1998) *Annu. Rev. Biochem.* **67,** 821–855
15. Kemp, B. E., Mitchelhill, K. I., Stapleton, D., Michell, B. J., Chen, Z. P., and Witters, L. A. (1999) *Trends. Biochem. Sci.* **24,** 22–25
16. Kahn, B. B., Alquier, T., Carling, D., and Hardie, D. G. (2005) *Cell. Metab.* **1,** 15–25
17. Long, Y. C., and Zierath, J. R. (2006) *J. Clin. Invest.* **116,** 1776–1783
18. Sanders, M. J., Grondin, P. O., Hegarty, B. D., Snowden, M. A., and Carling, D. (2007) *Biochem. J.* **403,** 139–148
19. Young, M. E., Radda, G. K., and Leighton, B. (1996) *FEBS Lett.* **382,** 43–47
20. Merrill, G. F., Kurth, E. J., Hardie, D. G., and Winder, W. W. (1997) *Am. J. Physiol.* **273,** E1107–E1112
21. Igata, M., Motoshima, H., Tsuruzoe, K., Kojima, K., Matsumura, T., Kondo, T., Taguchi, T., Nakamaru, K., Yano, M., Kukidome, D., Matsumoto, K., Toyonaga, T., Asano, T., Nishikawa, T., and Araki, E. (2005) *Circ. Res.* **97,** 837–844
22. Nagata, D., Takeda, R., Sata, M., Satonaka, H., Suzuki, E., Nagano, T., and Hirata, Y. (2004) *Circulation* **110,** 444–451
23. Jhun, B. S., Jin, Q., Oh, Y. T., Kim, S. S., Kong, Y., Cho, Y. H., Ha, J., Baik, H. H., and Kang, I. (2004) *Biochem. Biophys. Res. Commun.* **318,** 372–380
24. Chodakewitz, J. A., Kupper, T. S., and Coleman, D. L. (1988) *J. Immunol.* **140,** 832–836
25. Munker, R., Gasson, J., Ogawa, M., and Koeffler, H. P. (1986) *Nature* **323,** 79–82
26. Ouchi, N., Kobayashi, H., Kihara, S., Kumada, M., Sato, K., Inoue, T., Funahashi, T., and Walsh, K. (2004) *J. Biol. Chem.* **279,** 1304–1309
27. Sakoda, H., Ogihara, T., Anai, M., Fujishiro, M., Ono, H., Onishi, Y., Katagiri, H., Abe, M., Fukushima, Y., Shojima, N., Inukai, K., Kikuchi, M., Oka, Y., and Asano, T. (2002) *Am. J. Physiol. Endocrinol. Metab.* **282,** E1239–E1244
28. Senokuchi, T., Matsumura, T., Sakai, M., Yano, M., Taguchi, T., Matsuo, T., Sonoda, K., Kukidome, D., Imoto, K., Nishikawa, T., Kim-Mitsuyama, S., Takuwa, Y., and Araki, E. (2005) *J. Biol. Chem.* **280,** 6627–6633
29. Taketa, K., Matsumura, T., Yano, M., Ishii, N., Senokuchi, T., Motoshima, H., Murata, Y., Kim-Mitsuyama, S., Kawada, T., Itabe, H., Takeya, M., Nishikawa, T., Tsuruzoe, K., and Araki, E. (2008) *J. Biol. Chem.* **283,** 9852–9862
30. Campàs, C., Lopez, J. M., Santidrián, A. F., Barragán, M., Bellosillo, B., Colomer, D., and Gil, J. (2003) *Blood.* **101,** 3674–3680
31. Garcia-Gil, M., Pesi, R., Perna, S., Allegrini, S., Giannecchini, M., Camici, M., and Tozzi, M. G. (2003) *Neuroscience* **117,** 811–820
32. Imamura, K., Ogura, T., Kishimoto, A., Kaminishi, M., and Esumi, H. (2001) *Biochem. Biophys. Res. Commun.* **287,** 562–567
33. Jones, R. G., Plas, D. R., Kubek, S., Buzzai, M., Mu, J., Xu, Y., Birnbaum, M. J., and Thompson, C. B. (2005) *Mol. Cell.* **18,** 283–293
34. Sherr, C. J. (1996) *Science* **274,** 1672–1677
35. Graña, X., and Reddy, E. P. (1995) *Oncogene* **11,** 211–219
36. Hunter, T., and Pines, J. (1994) *Cell* **79,** 573–582
37. Shieh, S. Y., Ikeda, M., Taya, Y., and Prives, C. (1997) *Cell* **91,** 325–334
38. Rattan, R., Giri, S., Singh, A. K., and Singh, I. (2005) *J. Biol. Chem.* **280,** 39582–39593
39. Bode, A. M., and Dong, Z. (2009) *Nat. Rev. Cancer.* **4,** 793–805

Am J Physiol Endocrinol Metab 296: E842–E853, 2009.
First published January 27, 2009; doi:10.1152/ajpendo.90528.2008.

Role of the liver in glucose homeostasis in PI 3-kinase *p85α*-deficient mice

Kazutaka Aoki,[1] Junji Matsui,[2] Naoto Kubota,[2,3,4] Hiromu Nakajima,[5] Keiji Iwamoto,[2] Iseki Takamoto,[2,3,4] Youki Tsuji,[2] Akira Ohno,[6] Shuuichi Mori,[7] Kumpei Tokuyama,[7] Koji Murakami,[2] Tomoichiro Asano,[2] Shinichi Aizawa,[8] Kazuyuki Tobe,[2,3] Takashi Kadowaki,[2,3,4] and Yasuo Terauchi[1,2]

[1]*Department of Endocrinology and Metabolism, Yokohama City University Graduate School of Medicine, Yokohama;* [2]*Department of Metabolic Diseases, Graduate School of Medicine, University of Tokyo, Tokyo;* [3]*Core Research for Evolutional Science and Technology, Japan Science and Technology Corporation, Kawaguchi;* [4]*Division of Applied Nutrition, National Institute of Health and Nutrition, Tokyo;* [5]*Department of Laboratory Medicine, Osaka Medical Center for Cancer and Cardiovascular Diseases, Osaka;* [6]*Department of Medicine, Ikeda Municipal Hospital, Ikeda;* [7]*Graduate School of Comprehensive Human Sciences, University of Tsukuba, Tsukuba; and* [8]*Laboratory for Vertebrate Body Plan, Center for Developmental Biology, Institute of Physical and Chemical Research (RIKEN), Kobe, Japan*

Submitted 22 June 2008; accepted in final form 10 January 2009

Aoki K, Matsui J, Kubota N, Nakajima H, Iwamoto K, Takamoto I, Tsuji Y, Ohno A, Mori S, Tokuyama K, Murakami K, Asano T, Aizawa S, Tobe K, Kadowaki T, Terauchi Y. Role of the liver in glucose homeostasis in PI 3-kinase *p85α*-deficient mice. *Am J Physiol Endocrinol Metab* 296: E842–E853, 2009. First published January 27, 2009; doi:10.1152/ajpendo.90528.2008.—Phosphoinositide 3-kinase (PI3K) *p85α*-deficient mice exhibit hypoglycemia as a result of increased insulin sensitivity and glucose uptake in peripheral tissues. Although PI3K is central to the metabolic actions of insulin, its mechanism of action in liver is not well understood. In the present study, we investigated hepatic insulin signaling and glucose homeostasis in *p85α*-deficient and wild-type mice. In the livers of *p85α*-deficient mice, p50α played a compensatory role in insulin-stimulated PI3K activation by binding to insulin receptor substrate (IRS)-1/2. In *p85α*-deficient mice, the ratio of p50α over p110 catalytic subunit of PI3K in the liver was higher than in the muscles. PI3K activity associated with IRS-1/2 was not affected by the lack of *p85α* in the liver. Insulin-stimulated Akt and phosphatase and tensin homologue deleted on chromosome 10 (PTEN) activities in the liver were similar in *p85α*-deficient and wild-type mice. A hyperinsulinemic-euglycemic clamp study revealed that the glucose infusion rate and the rate of disappearance were higher in *p85α*-deficient mice than in wild-type mice but that endogenous glucose production tended to be higher in *p85α*-deficient mice than in wild-type mice. Consistent with this finding, the expression of glucose-6-phosphatase and phosphoenolpyruvate carboxykinase in livers after fasting was higher in *p85α*-deficient mice than in wild-type mice. After mice were fasted, the intrahepatic glucose-6-phosphate level was almost completely depleted in *p85α*-deficient mice. The glycogen content fell to nearly zero as a result of glycogenolysis shortly after the initiation of fasting in *p85α*-deficient mice. The absence of an increase in insulin-stimulated PI3K activation in the liver of *p85α*-deficient mice, unlike the muscles, may be associated with the molecular balance between the regulatory subunit and the catalytic subunit of PI3K. Gluconeogenesis was rather elevated in *p85α*-deficient mice, compared with in wild-type mice, and the liver seemed to partially compensate for the increase in glucose uptake in peripheral tissues.

phosphoinositide 3-kinase; regulatory subunit; catalytic subunit

DEFECTS IN INSULIN SECRETION from pancreatic β-cells and insulin resistance in the target tissues interact in a complex manner to disturb glucose homeostasis and cause type 2 diabetes (39, 40, 42, 47). Insulin activates phosphoinositide 3-kinase (PI3K) via the tyrosine phosphorylation of insulin receptor substrates (IRSs) and the subsequent binding of p85α associated with p110 (17, 18, 24, 28, 33, 34). Previous in vitro experiments (13, 32) have suggested that the activation of PI3K plays an important role in the metabolic actions of insulin, like glucose transporter (GLUT) translocation and glycogen synthase activation. To investigate the role of PI3K in glucose metabolism in vivo, we specifically deleted the first exon of *Pik3r1* in mice (exon 1A). Because this exon contains the initiation codon for p85α, we were able to selectively abolish the expression of full-length p85α mRNA without disrupting the p55α (2, 15) and p50α (8, 16) splicing variants. Mice deficient in p85α were born and showed no apparent growth abnormalities, presumably due to redundant PI3K activities (43). By contrast, the absence of all three isoforms of the p85α gene is reportedly a fatal condition during the perinatal period (9).

Mice deficient in *p85α* were hypoglycemic because of an increase in glucose uptake in peripheral tissues (43). The phenotype of *p85α*-deficient mice can be explained by an increase in the insulin-induced generation of phosphatidylinositol 3,4,5-triphosphate (PIP3) in association with an isoform switch from p85α PI3K to p50α PI3K in peripheral tissues. It should be noted, however, that the targeted disruption of p50α and p55α PI3K also led to increased insulin sensitivity (5). Recently, Taniguchi et al. (38) reported that mice with a liver-specific deletion of the p85α regulatory subunit exhibited a paradoxical improvement in hepatic and peripheral insulin sensitivity but that liver-specific deletions of both the p85α and the p85β regulatory subunits led to an increase in gluconeogenesis in association with the impairment of PI3K activation (37). In this context, Kahn and colleagues reported that the heterozygous disruption of the *Pik3r1* gene improved insulin signaling in liver and muscle (25) and hypothesized that optimal signaling through the PI3K pathway depended on a critical molecular balance between the regulatory and catalytic subunits (45). This hypothesis invokes the existence of non-p110-bound p85 ("free p85"), which can compete with the heterodimeric p85/p110, thereby dampening PI3K signaling. In this context, Vanhaesebroeck and colleagues (12) argued

Address for reprint requests and other correspondence: Y. Terauchi, Dept. of Endocrinology and Metabolism, Yokohama City Univ. Graduate School of Medicine, 3-9 Fukuura, Kanazawa-ku, Yokohama 236-0004, Japan (e-mail: terauchi@yokohama-cu.ac.jp).

The costs of publication of this article were defrayed in part by the payment of page charges. The article must therefore be hereby marked "*advertisement*" in accordance with 18 U.S.C. Section 1734 solely to indicate this fact.

against the free p85 hypothesis. Moreover, it has been reported that PTEN (phosphatase and tensin homologue deleted on chromosome 10) activity is decreased in p85α-null liver (38), raising the possibility that loss of expression of p85 affects lipid phosphatases. Thus although PI3K is central to the metabolic actions of insulin, its mechanism of action is not well understood. We therefore investigated the role of the liver in glucose homeostasis in *p85α*-deficient mice and the impact of molecular balance between the regulatory and catalytic subunits of PI3K on downstream signaling through the PI3K pathway.

MATERIALS AND METHODS

Animals and genotyping. Mice lacking *p85α* (C57Bl/6J and CBA mixed background) were generated as previously described (43). These mice were backcrossed with C57Bl/6J mice (CLEA Japan) or BALB/c mice (Taconic Farm; Ref. 11). Because the murine genetic background was not completely homogeneous, male offspring derived from $p85\alpha^{+/-}$ intercrosses were analyzed in this study. For the immunoblotting experiments, the PI3K activity assays, the Akt and PTEN assays, the hyperinsulinemic-euglycemic glucose clump study, the gluconeogenic activity in vivo, and the TaqMan PCR analysis, the male offspring derived from $p85\alpha^{+/-}$ intercrosses that were bred on a C57Bl/6J and BALB/c mixed background were used. For other experiments, mice on a C57Bl/6J background were used. Our experimental procedures were approved by the Institutional Ethics Committee of Yokohama City University, and then the experiments were performed in accordance with the guidelines of the Animal Care Committee of Yokohama City University. The mice were fed water and normal laboratory chow ad libitum and maintained using standard animal husbandry procedures. All mice were kept on a 12:12-h light-dark cycle.

The *Pik3r1* genotype was determined using PCR. Genomic DNA was extracted from the tip of the tail. The sense primer was PI-6 (5′-CAGATGGACAGTGTGACAGG-3′), and the antisense primers were PI-9 (5′-AGGGGGTGAAATTCTTTTCC-3′) for the *Pik3r1* gene and Neo-1 (5′-CCAGTCATAGCCGAATAGCC-3′) for a neomycin-resistance gene. The three primers and the genomic DNA template were mixed in a tube. The wild-type allele produced a 600-bp product, and the recombinant allele produced a 450-bp product.

Antibodies. Anti-p85 polyclonal antibody against a full-length p85-GST fusion protein containing the NH2-terminal SH2 domain of p85α (anti-$p85^{PAN}$) and anti-p110α antibody against the COOH-terminal region (aa 1,054–1,068; anti-p110α) were purchased from Upstate Biotechnology (Lake Placid, NY). Specific antibodies against p50α (anti-p50α), p55α (anti-p55α), p55γ (anti-p55γ), and p85β (anti-p85β) were generated as previously described (8, 16). The monoclonal anti-phosphotyrosine antibody (anti-PY), polyclonal anti-IRS-1 antibody (anti-IRS-1), and polyclonal anti-IRS-2 antibody (anti-IRS-2) were purchased from Upstate Biotechnology rabbit polyclonal anti-phospho-AKT antibody (anti-pAKT) recognizing phosphorylated Ser-473 of Akt1 and rabbit anti-Akt antibody (anti-AKT) were purchased from Cell Signaling Technology (Beverly, MA).

Immunoprecipitations and immunoblotting. The livers and muscles were excised and homogenized in ice-cold *buffer A* (25 mM Tris·HCl pH 7.4, 10 mM Na_3VO_4, 10 mM NaPPi, 100 mM NaF, 10 mM EDTA, 10 mM EGTA, and 1 mM PMSF). Lysates were prepared using centrifugation (15,000 rpm, 20 min, 4°C). Lysates containing equal amounts of total protein (~100 μg) were incubated with the indicated antibody for 1 h at 4°C and then with protein G-Sepharose for 1 h at 4°C. The beads were washed three times with *buffer A* containing 1% Triton X-100, and the immunoprecipitated proteins were solubilized with Laemmli's sample buffer. Samples were separated on SDS-polyacrylamide gels and transferred to nitrocellulose followed by immunoblotting with the indicated antibody. The blots were incubated with horseradish peroxidase-linked protein A, and the bands were detected using enhanced chemiluminescence (Amersham International, England, UK).

PI3K assay. PI3K activity in the liver was determined in immunoprecipitates using the indicated antibodies after insulin injection into the inferior vena cava (22, 48). PI3K was immunoprecipitated with the indicated antibody, and the immunoprecipitates were washed three times with *buffer A* containing 1% Triton X-100 and then three more times with PI3K reaction buffer (20 mM Tris-HCl pH 7.4, 100 mM NaCl, 1 mM Na_3VO_4, and 0.5 mM EGTA). The reaction was initiated by addition of 50 μl of PI3K reaction buffer containing 20 mM $MgCl_2$, 20 μM ATP, 5 μCi of [γ-^{32}P]ATP, and 0.2 mg/ml of phosphatidylinositol to the immunoprecipitates. After incubation at 25°C for 20 min, the reaction was terminated by the addition of 100 μl of chloroform containing HCl and the organic phase was separated by centrifugation and washed three times with methanol-1 M HCl (1:1). The lipids were spotted onto a Silicagel 60 plate (Merck, Darmstadt, Germany) and developed in chloroform, methanol, 28% ammonium hydroxide, and water (43:38:5:7). The phosphorylated lipids were visualized and evaluated using a BAS 2000 system (Fuji Film, Kanagawa, Japan).

Changes in expression of regulatory subunits of PI3K and PI3K activity associated with IRS-1 and IRS-2. Four-to-five-month-old male mice were subjected to fasting for 24 h or were refed for 6 h after a 24-h period of starvation. Hepatic lysates were incubated with antibody against IRS-1 or IRS-2 and then with protein G-Sepharose. Immunoblot analyses were then performed as described above. PI3K activity was measured after immunoprecipitation with IRS-1(n = 6) or IRS-2 (n = 5) antibodies using PI3K assay kit (Jena Biosciences, Jena, Germany). The radioactivity of sample was measured in the liquid scintillation counter.

In vivo insulin stimulation and analyses of Akt, pAkt, and PTEN. Four-month-old male mice were starved for 24 h, anesthetized with pentobarbital, and injected with 5 U of regular human insulin (Humalin R; Lilly) or saline into the inferior vena cava. Five minutes later, the livers were removed and homogenized in ice-cold *buffer A*. Immunoblot analyses for Akt and pAkt were then performed. Akt activity was expressed as the ratio of the intensity of pAkt to Akt.

To analyze PTEN activity, the livers were homogenized in ice-cold buffer (20 mM imidazol-HCl, 2 mM EDTA, 2 mM EGTA pH 7.0, containing 1 mM benzamidine, 0.8 μM aprotinin, 50 μM vestatin, 15 μM E-64, 20 μM leupeptin, and 10 μM pepstatin A) and measured using the PTEN malachite green assay kit (Upstate Biotechnology, Lake Placid, NY). PTEN activity was expressed as the activity per 1 mg protein of liver lysate.

Hyperinsulinemic-euglycemic clamp study. The clamp studies were carried out as described previously (20, 36), with slight modifications. Studies were performed using 4-to-5-mo-old male mice under conscious and unstressed conditions after a 6-h fast. A primed continuous infusion of insulin (Humalin R; Lilly) was given (5.0 $mU \cdot kg^{-1} \cdot min^{-1}$), and the blood glucose concentration, which was monitored every 5 min, was maintained at ~120 mg/dl through the administration of glucose (5 g of glucose per 10 ml, enriched to ~20% with D-glucose-6,6-d_2; Isotec) for 120 min. Blood was sampled via tail tip bleeds at 90, 105, and 120 min to determine the rate of glucose disappearance (R_d). R_d was calculated using nonsteady-state equations (36), and endogenous glucose production (EGP) was calculated as the difference between R_d and the exogenous glucose infusion rate (GIR; Ref. 36).

Gluconeogenic activity in vivo. Mice were subjected to fasting for 24 h or were refed for 6 h after a 24-h period of starvation. Gluconeogenic activity was measured using a previously described method (3, 10, 31). NaH[^{14}C]CO_3 (20 μCi/10 g body wt) was intravenously injected via the tail vein. Blood samples (100 μl) were then obtained at 20 min after NaH[^{14}C]CO_3 administration. The collected blood was hemolyzed in 1.2 m of distilled water and then deproteinized through

the addition of 0.1 ml of 0.3 M $Ba(OH)_2$ and 0.1 ml of 0.3 M $ZnSO_4$, followed by centrifugation at 9,000 rpm for 5 min. To evaluate the total infusion quantity, the radioisotopes in 0.1 ml of the supernatant were counted using a liquid scintillation counter and PICO-FLUOR 40 solvent (Packard Bio Science). Each preparation of the supernatant was divided into two tubes, each containing 0.47 ml, and then 10 μl of 0.5 M adenosine triphosphate and 20 μl of 8.4% bicarbonate were added to each tube. Five units of hexokinase (Wako Pure Chemical Industries) were added to one of each pair of tubes. After 30 min of incubation at 37°C, 450 μl of supernatant with or without hexokinase were placed into a tube containing anion-exchange resin (AG-8X, form, 200–400 mesh; Bio-Rad, Hercules, CA) overnight at 37°C. After centrifugation at 6,000 rpm for 10 min, the radioactivity of each sample was measured using a liquid scintillation counter. The gluconeogenic activity was expressed as the ratio of [^{14}C]glucose, which is the difference between the radioactivity in the sample with and that in the sample without hexokinase compared with the total infusion radioactivity.

TaqMan PCR. Four-month-old male mice were subjected to fasting for 24 h or were refed for 6 h after a 24-h period of starvation. Total RNA was prepared from portions of the liver using Isogen reagent (NipponGene, Tokyo) according to the manufacturer's instructions. The mRNA levels in the liver were quantitatively analyzed using fluorescence-based reverse transcriptase-PCR. The reverse transcription mixture was amplified using specific primers and an ABI Prism 7000 sequence detector equipped with a thermocycler. The primers used for glucose-6-phosphatase (G6Pase), phospho*enol*pyruvate carboxykinase (PEPCK), and glucokinase (GK) were purchased from Applied Biosystems (Foster City, CA). The primers used for β-actin were described previously (21). The relative expression levels were compared after normalization to β-actin.

Measurement of serum parameters. Glucose levels were measured using a glucose test sensor (SKK, Nagoya, Japan). Insulin levels were determined using an insulin kit (BioTrak, Amersham Life Science) with rat insulin as the standard. To determine the lactate and pyruvate levels, trunk blood was extracted with an equivalent amount of perchloric acid (6%). Serum lactate, pyruvate, total cholesterol, and triglyceride levels were determined using Determiner-LA, -PA, -TC, and -TG kits, respectively (Kyowa Medex, Japan). Serum glycerol levels were determined using the Determiner-TG kit. Serum free fatty acid levels were determined using a commercial kit (Wako Chemicals, Osaka, Japan). Serum levels of amino acids, like alanine and glutamine, were measured using enzyme assays and HPLC. Plasma cAMP levels were determined using a commercial kit (Mikasa).

Measurement of gluconeogenic and glycolytic intermediates in the liver. Portions of the liver were removed from freely fed or 24-h-fasted male mice and were immediately frozen in liquid nitrogen. The levels of glucose metabolites were then determined as described previously (4).

Measurement of glycogen content. After portions of the liver had been lysed with 30% KOH and precipitated with ethanol, the glycogen content was measured using Anthron/H_2SO_4.

Statistical analysis. Results were expressed as the means ± SE. Statistical differences were analyzed using the Student *t*-test for unpaired comparisons. A Tukey-Kramer test was used for comparisons among four groups of mice. A P value < 0.05 was considered statistically significant.

RESULTS

Isoform switch from p85α to p50α in insulin-stimulated activation of PI3K. We first investigated PI3K activities in hepatic lysates stimulated with insulin and immunoprecipitated with anti-phosphotyrosine antibody (anti-PY) or anti-IRS-1 antibody (anti-IRS-1). Despite the complete abrogation of the p85α molecule, hepatic PI3K activity in the anti-PY immunoprecipitates was normal (Fig. 1*A*), and similar results were obtained with anti-IRS-1 (data not shown). We next investigated the expression levels of hepatic PI3K regulatory subunit isoforms (Fig. 1*B*). Lysates were immunoprecipitated with a panel of antibodies against either the NH_2-terminal SH2 domain of p85 (anti-p85^{PAN}), which can recognize p85α as well as p50α, p55α, p55γ, and p85β; the p110α catalytic subunit of PI3K, or p50α, followed by blotting with anti-p85^{PAN}, or p50α. In wild-type mice, p85α was the major PI3K regulatory subunit isoform (Fig. 1*B*, *lane 1*) that bound to the p110α catalytic subunit (Fig. 1*B*, *lane 3*). In *p85α*-deficient mice, however, p50α was the major PI3K regulatory subunit isoform (Fig. 1*B*, *lanes 2*, *4*, and *5*) that bound to the p110α catalytic subunit (Fig. 1*B*, *lane 4*). The expression level of p50α was significantly higher in livers from *p85α*-deficient mice than that from wild-type mice (Fig. 1*B*, *lane 1* vs. *2*; see Fig. 2*A* for quantitative analysis). Hepatic p55γ was not detected in either mouse type when blotted with a specific antibody against p55γ (data not shown). The expression of p85β did not differ between wild-type and *p85α*-deficient mice (data not shown), and p85β association with p110 was weaker than the association between p50α and p110, which seemed to be predominant (Fig. 1*B*, *lane 4*). Since IRS-1/2 protein is tyrosine-phosphorylated in response to insulin stimulation, we determined which regulatory subunits were bound to IRS proteins in vivo in response to insulin. IRS-1 was tyrosine phosphorylated, to similar extents, in both wild-type and *p85α*-deficient mice (Fig. 1*C*, *top*). The lysates were immunoprecipitated with anti-IRS-1 and blotted with anti-p85^{PAN}. In wild-type mice, p85α was bound to IRS-1 in an insulin-dependent fashion in these tissues. In *p85α*-deficient mice, p50α was the major protein recognized by anti-p85^{PAN} bound to IRS-1 in an insulin-dependent fashion (Fig. 1*C*, *middle* and *bottom*). IRS-2 was also tyrosine-phosphorylated, to similar extents, in both wild-type and *p85α*-deficient mice (Fig. 1*D*, *top*). The lysates were immunoprecipitated with anti-IRS-2 and blotted with anti-p85^{PAN}. In wild-type mice, p85α was bound to IRS-2 in an insulin-dependent fashion in these tissues. In *p85α*-deficient mice, p50α was the major protein recognized by anti-p85^{PAN} bound to IRS-2 in an insulin-dependent fashion (Fig. 1*D*, *middle* and *bottom*). When the immunoprecipitation and immunoblotting were carried out in a reverse manner, IRS-1 was found to be the tyrosine-phosphorylated protein bound to p85α in wild-type mice and to p50α in *p85α*-deficient mice after insulin stimulation of the liver (Fig. 1*E*). IRS-2 was also associated with p85α in wild-type mice and p50α in *p85α*-deficient mice after insulin stimulation of the liver (Fig. 1*E*). The binding of p50α to IRS-1/2 was stronger in *p85α*-deficient mice than in wild-type mice (Fig. 1*E*, *bottom*). We thus concluded that p85α in wild-type mice and p50α in *p85α*-deficient mice play a major role in insulin-stimulated PI3K activation via binding to the IRS family of proteins in the liver.

We (43) previously reported that the expression of p50α was much lower than that of p85α in muscles from wild-type mice. We now performed a direct comparison of the regulatory and catalytic subunits of PI3K in liver and muscles. In wild-type mice, the expression of p50α in liver was much higher than in the muscles (Fig. 2*A*). The expression level of p50α in the liver of *p85α*-deficient mice was significantly higher than that of wild-type mice (Fig. 2*A*). Interestingly, the expression level of p110α in the liver of *p85α*-deficient mice was lower than that

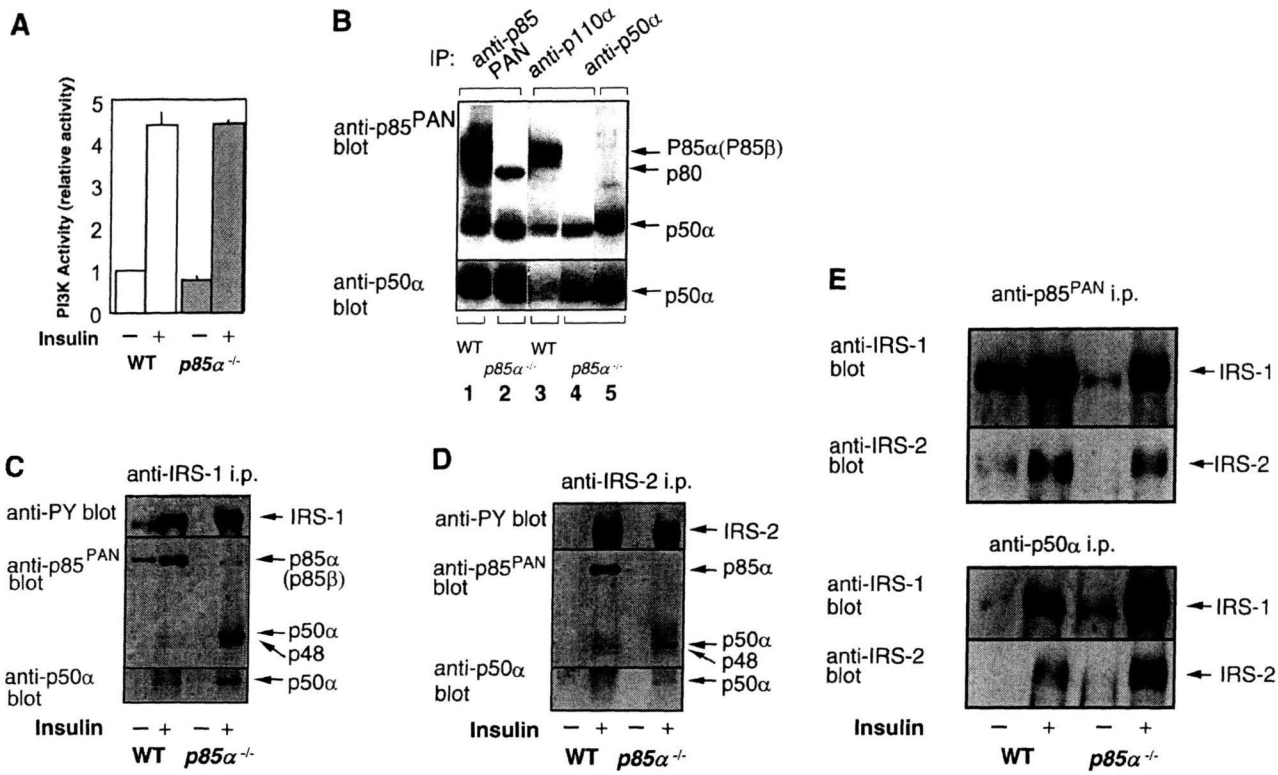

Fig. 1. Switch in phosphoinositide 3-kinase (PI3K) regulatory subunit isoform from p85α to p50α in the liver. *A*: PI3K activities associated with tyrosine-phosphorylated proteins. PI3K activities in the lysates were determined using anti-phosphotyrosine (anti-PY) immunoprecipitates. In each experiment, the PI3K activity was determined relative to that measured in wild-type mice under basal conditions. Results are means ± SE of 6 experiments in wild-type (WT) or *p85α*-deficient ($p85\alpha^{-/-}$) mice. *B*: expression of regulatory subunits of PI3K. Lysates from the liver were directly immunoprecipitated (IP) with anti-$p85^{PAN}$, anti-p110α, or anti-p50α and blotted with anti-$p85^{PAN}$ (*top*) or anti-p50α (*bottom*). Typical images are shown. *C*: PI3K regulatory subunits bound to insulin receptor substrate (IRS)-1. Lysates from liver with or without insulin stimulation were immunoprecipitated with anti-IRS-1 and blotted with anti-PY (*top*), anti-$p85^{PAN}$ (*middle*), or anti-p50α (*bottom*). Typical images of more than 3 experiments are shown. In some knockout animals, another 85-kD protein, presumably p85β, was bound to IRS-1, although the relative amount of this protein was much lower than that of p50α. We also noted a 48-kDa protein recognized by anti-$p85^{PAN}$ that bound to IRS-1, although the identity of this protein is presently unknown. *D*: PI3K regulatory subunits bound to IRS-2. Lysates from liver with or without insulin stimulation were immunoprecipitated with anti-IRS-2 and blotted with anti-PY (*top*), anti-$p85^{PAN}$ (*middle*), or anti-p50α (*bottom*). Typical images of more than 3 experiments are shown. We also noted a 48-kDs protein recognized by anti-$p85^{PAN}$ that bound to IRS-2, although the identity of this protein is presently unknown. *E*: IRS-1/2 bound to PI3K regulatory subunits. Lysates from liver with or without insulin stimulation were immunoprecipitated with anti-$p85^{PAN}$ (*top*) or anti-p50α (*bottom*) and blotted with anti-IRS-1 or anti-IRS-2. Typical images of >3 experiments are shown.

of wild-type mice (Fig. 2*B*). The expression level of p110α in the muscles of *p85α*-deficient mice tended to be lower than that of wild-type mice, although the difference was not statistically significant (Fig. 2*B*). Therefore, in *p85α*-deficient mice, the ratio of p50α over p110 in liver was higher than that in muscles, suggesting that the molecular balance between the regulatory subunit and the catalytic subunit of PI3K was different between the two tissues.

Expression of regulatory subunits of PI3K and PI3K activity associated with IRS-1 and IRS-2 during fasting and feeding. We (19) recently proposed the concept of the existence of a dynamic relay between IRS-1 and IRS-2 in hepatic insulin signaling during fasting and feeding. We therefore examined the expression of IRS-1/2 and the regulatory subunit of PI3K and PI3K activity associated with IRS-1/2 during fasting and feeding (6 h). In wild-type mice, the expression of p85α associated with IRS-1 was not different under fasted or refed conditions (Fig. 3*A*). By contrast, the expression of p85α associated with IRS-2 under fasted conditions was decreased compared with refed conditions (Fig. 3*B*). Under refed conditions, the expression of p50α associated with IRS-1/2 was increased in *p85α*-deficient mice compared with wild-type mice (Fig. 3, *A* and *B*). PI3K activities associated with IRS-1 tended to be increased under refed conditions compared with fasted conditions, although the difference was not statistically significant (Fig. 3*C*). No significant differences in PI3K activities were observed under either fasted or refed conditions after immunoprecipitating with IRS-2 antibodies (Fig. 3*D*). These results were essentially consistent with our previous study (19), and IRS-1/2 associated PI3K activity was not affected by the lack of *p85α* in the liver. The expression of IRS-1 and IRS-2 was increased in *p85α*-deficient mice under fasted conditions, compared with wild-type mice (data not shown).

Akt and PTEN activities. No significant difference in insulin-stimulated Akt activity, which was measured according to Ser-473 phosphorylation, was observed between wild-type and *p85α*-deficient mice (Fig. 4*A*). Furthermore, no significant difference in PTEN activity was observed between wild-type and *p85α*-deficient mice (Fig. 4*B*).

Hyperinsulinemic-euglycemic clamp study. We determined the metabolic response to high concentration of insulin. The

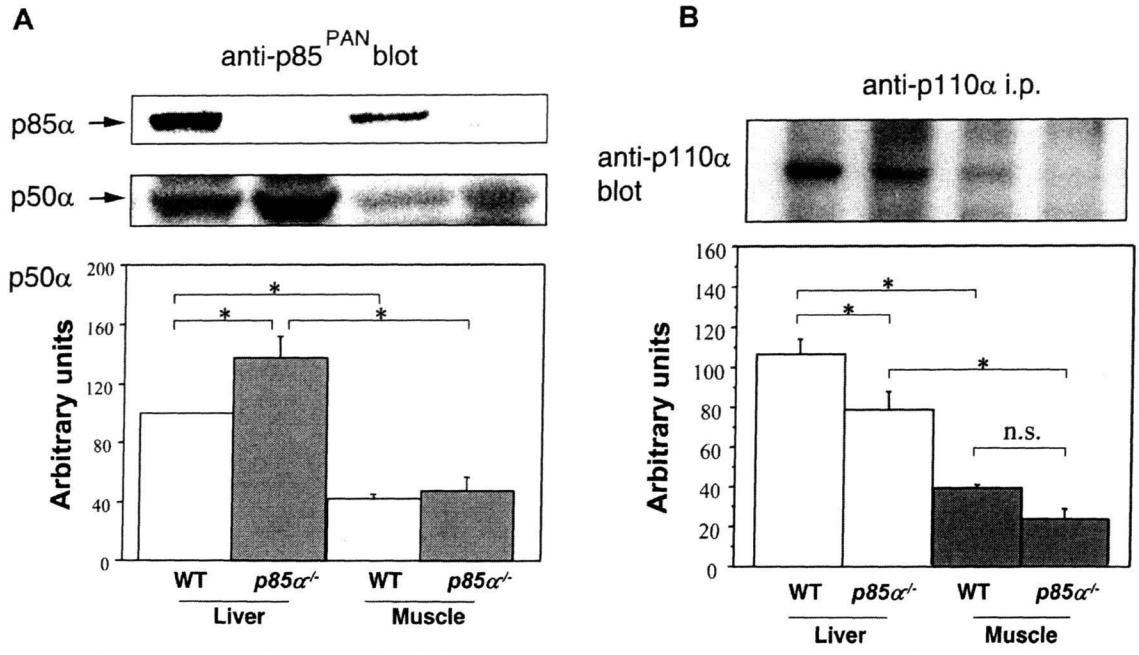

Fig. 2. Expression of regulatory and catalytic subunit of PI3K in the liver and muscle. *A*: expression of regulatory subunits of PI3K. Same amount of lysates (50 μg) from liver and muscle were immunoblotted with anti-$p85^{PAN}$. Expression level of p50α was quantified. *B*: expression of p110α. Lysates from the liver and muscle were directly immunoprecipitated with anti-p110α and then immunoblotted with anti-p110α. Each blot was quantified and shown in figures. Values are means ± SE. $*P < 0.05$.

GIR and R_d were significantly higher in *p85α*-deficient mice than in wild-type mice (Fig. 5, *A* and *C*). These results agreed with previous reports (43) that *p85α*-deficient mice exhibit increased insulin sensitivity in muscles and adipose tissue. It should be noted, however, that EGP tended to be higher in the *p85α*-deficient mice (by 27%) than in wild-type mice, although the difference was not statistically significant (Fig. 5*B*). These findings suggest that the insulin response was not improved in the livers of *p85α*-deficient mice.

Gluconeogenic activity in vivo. Figure 6 shows the total gluconeogenic activity in wild-type and *p85α*-deficient mice. No significant differences in glucose production were observed between the two mouse groups under either fasted or refed conditions. This result was consistent with the EGP results in the glucose-clamp study (Fig. 5).

Expression of genes involved in the hepatic glycolysis/gluconeogenesis pathways. We next examined the expression levels of G6Pase, PEPCK, and GK in the liver. The G6Pase mRNA levels were significantly higher (by 99%) in *p85α*-deficient mice than in wild-type mice under fasted conditions (Fig. 7*A*). The PEPCK mRNA levels were also significantly higher (by 62%) in *p85α*-deficient mice than in wild-type mice under fasted conditions (Fig. 7). After 6 h of refeeding after a 24-h fast, the G6Pase and PEPCK gene expression levels were lower in both wild-type and *p85α*-deficient mice than in the respective mouse groups after fasting. No significant differences in the expression of G6Pase and PEPCK were observed between *p85α*-deficient and wild-type mice under refed conditions (Fig. 7, *A* and *B*). GK expression in *p85α*-deficient mice tended to be higher than that in wild-type mice, although the difference was not statistically significant (Fig. 7C).

Depleted hexoses in livers of p85α-deficient mice under fasted conditions. Glucose is produced in the liver and renal cortex from nonglucose precursors through the process of gluconeogenesis. In *p85α*-deficient mice, the serum levels of nonglucose precursors, such as alanine, glutamine, pyruvate, lactate, and glycerol, were unaltered (Table 1), suggesting that sufficient supplies for gluconeogenesis were available from peripheral tissues. The serum corticosterone levels were 164 ± 18 ng/ml ($n = 5$) in wild-type mice and 156 ± 63 ng/ml ($n = 5$) in *p85α*-deficient mice (NS), indicating that the adrenal cortex function, which is necessary for gluconeogenesis in mice, was normal in the *p85α*-deficient mice. The serum levels of catecholamines were not reduced in *p85α*-deficient mice. Rather, the serum glucagon level was significantly higher in *p85α*-deficient mice than in wild-type mice under both fed and fasted conditions (Table 1).

The levels of intrahepatic intermediates involved in the gluconeogenic and glycolytic pathways in freely fed or 24-h-fasted wild-type and *p85α*-deficient mice are summarized in Table 2. Under fasted conditions in *p85α*-deficient mice, the G6Pase level was almost completely depleted and the fructose-6-phosphate level tended to be reduced, although the difference was not statistically significant. Under fed conditions, the G6Pase and phosphoenolpyruvate levels were higher in *p85α*-deficient mice than in wild-type mice, while the 2-phosphoglycerate level was lower in *p85α*-deficient mice than in wild-type mice.

Glycogen depletion in livers from p85α-deficient mice shortly after a fast. Glycogen deposition and glycogenolysis in the liver play pivotal roles in glucose homeostasis. Under freely fed conditions, the total amount of glycogen stored in the liver was lower, although not significantly, in *p85α*-deficient

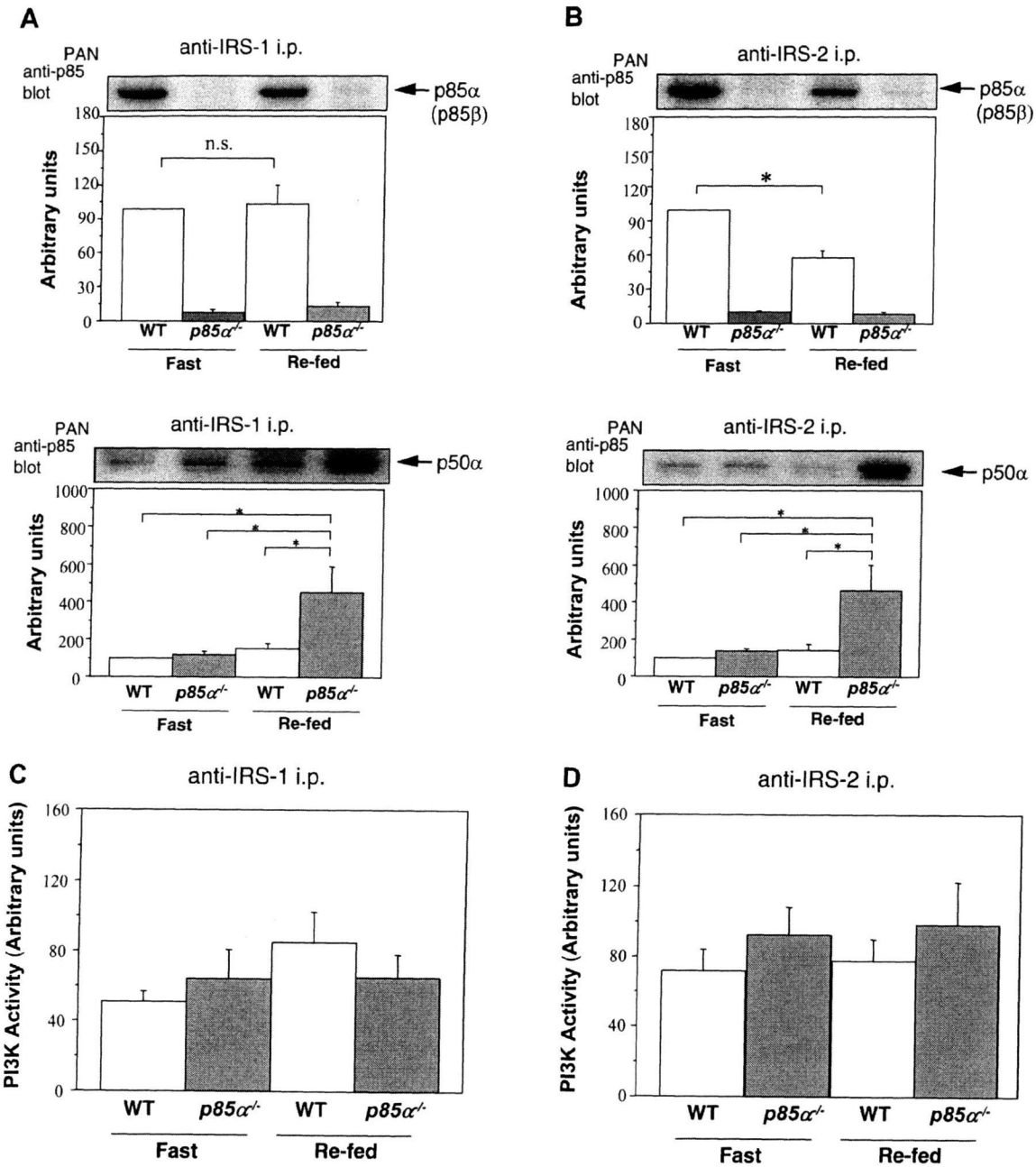

Fig. 3. Changes in expression of regulatory subunits of PI3K and PI3K activity associated with IRS-1 and IRS-2 during fasting and refeeding. Expression of p85α and p50α associated with IRS-1 (*A*) or IRS-2 (*B*). Mice were subjected to fasting for 24 h or were refed for 6 h after a 24-h period of starvation. Expression of p85α in the lysates were determined using anti-IRS-1 ($n = 4$) or IRS-2 ($n = 4$) immunoprecipitates. PI3K activity associated with IRS-1 (*C*) or IRS-2 (*D*). PI3K activity in lysates was determined using anti-IRS-1 ($n = 6$) or IRS-2 ($n = 5$) immunoprecipitates. Results are means ± SE in WT or $p85\alpha$-deficient ($p85\alpha^{-/-}$) mice. $^*P < 0.05$.

mice than in wild-type mice (Fig. 8*A*). The glycogen content fell to nearly zero via glycogenolysis in $p85\alpha$-deficient mice after a 12-h fast, while it was not completely depleted in wild-type mice even after a 30-h fast (Fig. 8*A*). The plasma cAMP level is known to increase in response to glucagon, which stimulates glycogenolysis by converting phosphorylase from an inactive form to an active form. When we injected glucagon into freely fed wild-type and $p85\alpha$-deficient mice, the changes in the plasma cAMP levels were indistinguishable (Fig. 8*B*). A similar result was obtained when the two types of mice were loaded with isoproterenol (Fig. 8*C*). Although glycogen stored in the liver was broken down more rapidly in $p85\alpha$-deficient mice than in wild-type mice in response to glucagon, the increments in circulating blood glucose were disproportionately small (Fig. 8*D*).

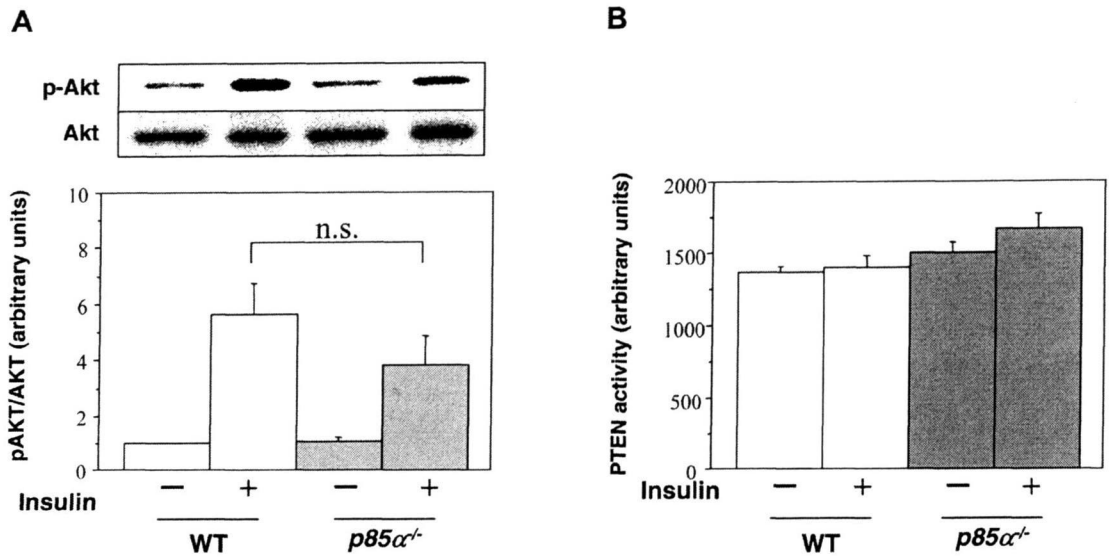

Fig. 4. Akt and PTEN activities in WT and $p85\alpha$-deficient mice ($p85\alpha^{-/-}$). *A*: Ser-473 phosphorylation of Akt (pAkt) and Akt were measured using western immunoblotting in WT ($n = 6$) and p85α-deficient mice ($n = 6$). Typical images are shown (*top*). Akt activities are expressed as the raito of pAkt to Akt (*bottom*). *B*: the phosphatase and tensin homologue deleted on chromosome 10 (PTEN) activities were measured using liver homogenates from WT ($n = 6$) and p85α-deficient mice ($n = 6$). Values are means ± SE.

DISCUSSION

In this study, we report four novel findings. First, insulin-stimulated PI3K activity associated with IRS in the liver was mediated via full-length p85α in wild-type mice and via the p50α alternative splicing isoform of the same gene in $p85\alpha$-deficient mice. In $p85\alpha$-deficient mice, the ratio of p50α over p110 in liver was higher than that in muscles, suggesting that the molecular balance between the regulatory subunit and the catalytic subunit of PI3K was different between the two tissues. Insulin-stimulated Akt and PTEN activities in the liver were similar in $p85\alpha$-deficient and wild-type mice. Second, a hyperinsulinemic-euglycemic clamp study revealed that GIR and R_d were higher in $p85\alpha$-deficient mice than in wild-type mice, consistent with a previous report (43) describing an increased sensitivity in muscles. By contrast, EGP tended to be higher in the $p85\alpha$-deficient mice than in wild-type mice, although the difference was not statistically significant. Moreover, under fasted conditions, the hepatic expression of G6Pase and PEPCK was higher in $p85\alpha$-deficient mice than in wild-type mice. Third, under fasted conditions, the intrahepatic G6Pase level was almost completely depleted and the fructose-6-phosphate tended to be reduced in $p85\alpha$-deficient mice. Fourth, glycogenolysis was not lower in $p85\alpha$-deficient mice than in wild-type mice. The glycogen profiles suggested that glucose utilization was increased in peripheral tissues or that glucose turnover was increased in vivo, consistent with a previous report (43) describing an increased glucose uptake in the peripheral tissues of $p85\alpha$-deficient mice. Thus the liver did not exacerbate hypoglycemia but rather partially compensated for the extraordinary increase in glucose uptake in peripheral tissues to maintain glucose homeostasis in $p85\alpha$-deficient mice.

Interestingly, insulin action was improved in the muscles, but not in the liver, of $p85\alpha$-deficient mice (Fig. 5, *A–C*). We hypothesize that the absence of an increase in insulin-stimulated PI3K activation in the liver can be explained by the molecular balance between the regulatory subunit and the catalytic subunit of PI3K

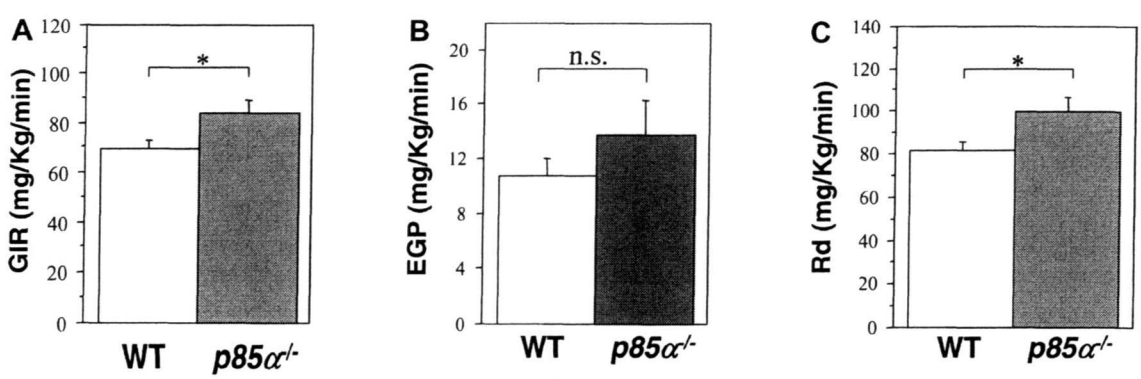

Fig. 5. Hyperinsulinemic-euglycemic clamp analysis in WT and $p85\alpha$-deficient mice ($p85\alpha^{-/-}$). Glucose infusion rate (GIR; *A*), endogenous glucose production (EGP; *B*), and rates of rate of glucose disappearance (R_d; *C*) in WT ($n = 9$) and $p85\alpha$-deficient mice ($n = 9$). Values are means ± SE. $^*P < 0.05$.

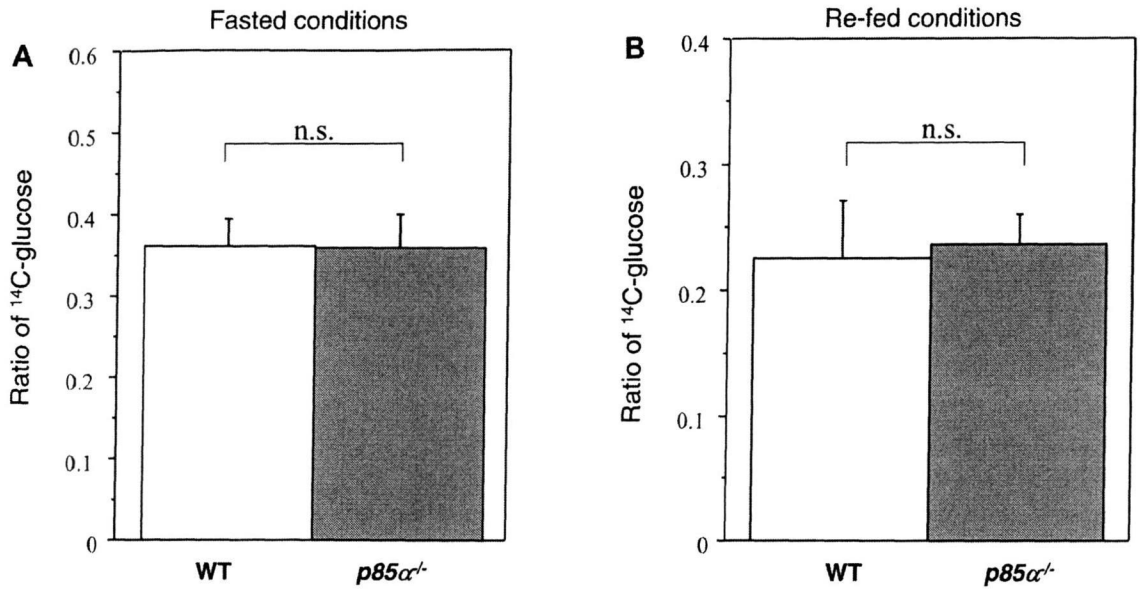

Fig. 6. Gluconeogenic activity in vivo. Total gluconeogenic activity in WT (n = 6) and $p85\alpha$-deficient mice (n = 6) is shown. Values are means ± SE.

in $p85\alpha$-deficient mice, as discussed by Taniguchi et al. In $p85\alpha$-deficient mice, p50α played a role in insulin-stimulated PI3K activation by binding to IRS-1/2. Although p50α was expressed in both wild-type and $p85\alpha$-deficient mice, the expression of p50α was much lower than that of p85α in the muscles of wild-type mice (43). We actually performed a direct comparison of the regulatory and catalytic subunits of PI3K in liver and muscles and noted that in $p85\alpha$-deficient mice, the ratio of p50α over p110 in liver was higher than that in muscles (Fig. 2*A*). These results suggested that the molecular balance between the regulatory subunit and the catalytic subunit of PI3K was different between the two tissues.

Based on experimental findings in adipocytes, we previously assumed that p50α might have a more potent effect on PI3K activation in vivo than p85α (43). It should be noted, however, that p50α/p55α-knockout mice exhibited enhanced insulin sensitivity (5). Moreover, Ueki et al. (44) reported that an increase in the expression level of p85α but not of p50α inhibited both phosphotyrosine-associated and p110-associated PI3-kinase activities in vitro (44), and they (45) proposed that optimal signaling through the PI3K pathway depended on a critical molecular balance between the regulatory and catalytic subunits. With the assumption that p50α has a more potent effect on PI3K activation than p85α in the liver, $p85\alpha$-deficient mice should have a lower EGP than wild-type mice. However, EGP tended to be higher in the $p85\alpha$-deficient mice than in wild-type mice. Indeed, no significant differences in PI3K activities associated with IRS-1/2 were observed under either fasted or refed conditions (Fig. 3, *C* and *D*). Together, the previous reports and the present study suggest that p50α is not more potent than p85α with respect to the activation of PI3K and that optimal signaling through the PI3K pathway depends on a critical molecular balance between the regulatory and catalytic subunits, although we were unable to directly address the free p85 hypothesis (45). Theoretically, decreased PTEN activity due to less p85-p110 bound to phosphorylated IRS molecule can explain the increased PIP3 generation in response to insulin (38), but insulin-stimulated PTEN activity was unaffected in liver of $p85\alpha$-deficient mice.

How can we understand glucose metabolism in the livers of $p85\alpha$-deficient mice? The expression of G6Pase and PEPCK was higher in $p85\alpha$-deficient mice than in wild-type

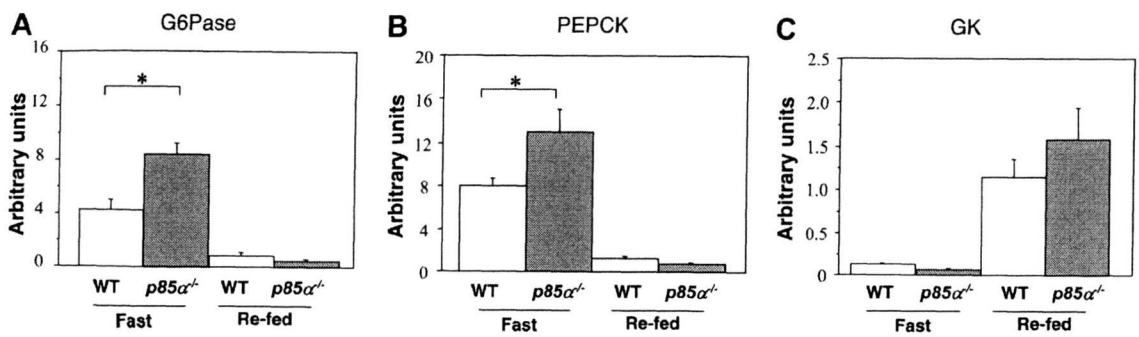

Fig. 7. Gene expression levels in WT and $p85\alpha$-deficient mice ($p85\alpha^{-/-}$). glucose-6-phosphatase (G6Pase; *A*), phospho*enol*pyruvate carboxykinase (PEPCK; *B*), and glucokinase (GK; *C*) expression in the livers of WT (n = 6) and $p85\alpha$-deficient mice (n = 6) are shown. Mice were subjected to fasting for 24 h or were refed for 6 h after a 24-h period of starvation. Expression levels were compared after normalization to β-actin level. Values are means ± SE. *$P < 0.05$.

Table 1. *Serum levels of lipids, gluconeogenic precursors, and hormones that promote gluconeogenesis*

	Fed		Fasted	
	Wild-type mice	Knockout mice	Wild-type mice	Knockout mice
Cholesterol, mg/dl	ND	ND	30.1±4.0 (4)	32.8±4.0 (5)
Triglyceride, mg/dl	ND	ND	40.4±4.9 (4)	59.4±12.1 (5)
Glycerol, mg/dl	ND	ND	41.6±2.0 (4)	48.0±4.9 (5)
Lactate, mg/dl	26.6±4.3 (9)	29.0±4.8 (9)	17.8±7.0 (5)	13.9±4.1 (5)
Pyruvate, mg/dl	1.000±0.084 (5)	0.982±0.99 (5)	1.024±0.268 (5)	0.908±0.263 (5)
Free fatty acid, mEq/l	0.820±0.126 (5)	1.076±0.417 (5)	1.335±0.249 (4)	1.028±0.224 (5)
Alanine, nanomol/ml	346±32 (5)	474±55 (5)	206±20 (4)	306±91 (5)
Glutamine, nanomol/ml	594±59 (5)	656±56 (5)	665±36 (4)	590±26 (5)
Insulin, ng/ml	0.26±0.06 (9)	0.14±0.05 (8)	0.16±0.04 (8)	0.06±0.02* (7)
Glucagon, ng/ml	1.13±0.19 (6)	2.40±0.50* (6)	0.96±0.22 (8)	2.19±0.32* (8)
Epinephrine, pg/ml	2.40±0.72 (3)	2.47±0.57 (3)	ND	ND
Norepinephrine, pg/ml	1.83±0.39 (3)	2.40±0.10 (3)	ND	ND

Data are means ± SE; n = no. of animals. Significant differences are indicated as $*P < 0.05$ for comparisons between wild-type and knockout mice under the same conditions. ND, not determined.

mice under fasted conditions. Because the G6Pase and PEPCK genes are reportedly controlled by insulin via the downstream PI3K signal (1, 7, 26, 35), the decreased serum insulin level (Table 1) may upregulate the expression of these gluconeogenic enzymes. Possibly, the reduction in serum insulin may have led to a reduction in insulin action in the central nervous system, thereby downregulating the gluconeogenic pathway (23, 30). Insulin and glucagon are known to have antagonistic actions on the expression of genes encoding all of the key enzymes involved in the glycolytic and gluconeogenic pathways (28). Thus glucagon has actions that oppose insulin by increasing hepatic cAMP. In this respect, the relatively high glucagon-to-insulin ratio in *p85α*-deficient mice (Table 1) may indicate the inhibition of glycolysis and the noninhibition or even enhancement of gluconeogenesis. Moreover, because *p85α*-deficient mice have a body weight and fat mass similar to those of wild-type mice, but significantly higher serum leptin levels when fed a normal diet (41), ablation of *p85α* may alter insulin/leptin signaling and their actions in the hypothalamus. To further understand the involvement of these molecules in glucose metabolism and the pertinent regulatory mechanisms, insulin action in the hypothalamus and the contribution of glucagon to the gluconeogenic pathway in the livers of *p85α*-deficient mice must be investigated. If the blockade of glucagon action in the livers of *p85α*-deficient mice leads to the downregulation of G6Pase and PEPCK, the increased glucagon level might play a major role in the regulation of gluconeogenesis. Otherwise, the contribution of the hypothalamus via insulin action may be important, and involvement of PI3K in the hypothalamus in the regulation of glucose metabolism in the liver should be intensively investigated.

Table 2. *Intrahepatic substrates in the glucose metabolic pathway*

	Fed Conditions		Fasted Conditions	
	Wild-type mice (n = 4)	Knockout mice (n = 3)	Wild-type mice (n = 3)	Knockout mice (n = 3)
Glucose	1.506±0.075	1.268±0.190	0.987±0.084†	1.069±0.330
G-1-P	0.035±0.002	0.038±0.009	0.026±0.001†	0.026±0.012
G-6-P	0.317±0.031	0.505±0.051*	0.340±0.062	0.022±0.003†‡
F-6-P	0.098±0.008	0.107±0.009	0.057±0.022†	0.010±0.003‡
F-1,6-P2	0.019±0.006	0.005±0.004	0.006±0.003	0.000±0.000
GAP	0.030±0.005	0.028±0.012	0.017±0.012	0.000±0.000
2PG	0.015±0.002	0.005±0.003*	0.006±0.002†	0.011±0.005
PEP	0.039±0.005	0.072±0.010*	0.071±0.018	0.049±0.016
Pyruvate	0.043±0.012	0.011±0.007	0.029±0.007	0.019±0.004

Amounts of intrahepatic substrates are expressed as means ± SE (μmol/g liver). G-1-P, glucose-1-phosphate; G-6-P, glucose-6-phosphate; F-6-P, fructose-6-phosphate; F-1,6-P2, fructose-1,6-bisphosphate; GAP, glyceraldehyde-3-phosphate; 2PG, 2-phosphoglycerate; PEP, phosphoenolpyruvate. Significant differences are indicated as $*P < 0.05$, $†P < 0.01$ for comparisons between wild-type and knockout mice under same conditions or $‡P < 0.05$ for comparisons between fed and fasted conditions in mice with same genotype.

The liver has been suggested to be capable of responding to hypoglycemia in the absence of any ability to secrete counterregulatory hormones or neural pathways between the liver and the brain (27). Normal mongrel dogs subjected to troglitazone treatment were shown to increase their endogenous glucose production in the liver as a result of elevations in both gluconeogenesis and glycogenolysis (6). The authors hypothesized that a protective mechanism existed in normal animals, preventing hypoglycemia during insulin sensitization with troglitazone. Thus increased glucose utilization in the peripheral tissues may itself, at least in part, upregulate gluconeogenic enzymes like G6Pase and PEPCK, thereby preventing severe hypoglycemia in *p85α*-deficient mice under fasted conditions. Recently, however, involvement of the liver in glucose metabolism in other tissues via the neuronal network has been suggested (14, 46). In this context, it should be noted that a liver-specific deletion of the p85α regulatory subunit, in which p50α was also abrogated, resulted in improvement in peripheral insulin sensitivity (38). This may be, at least in part, due to the neuronal network between liver and peripheral tissues. The results of our study can be interpreted that the liver partially compensated for the increase in glucose uptake in peripheral tissues to maintain glucose homeostasis in *p85α*-deficient mice but that the neuronal information pathway between the liver and peripheral tissues should be investigated in the future.

In summary, p50α played a role in insulin-stimulated PI3K activation by binding to hepatic IRS-1/2 in *p85α*-deficient mice. PI3K activity associated with IRS-1/2 was

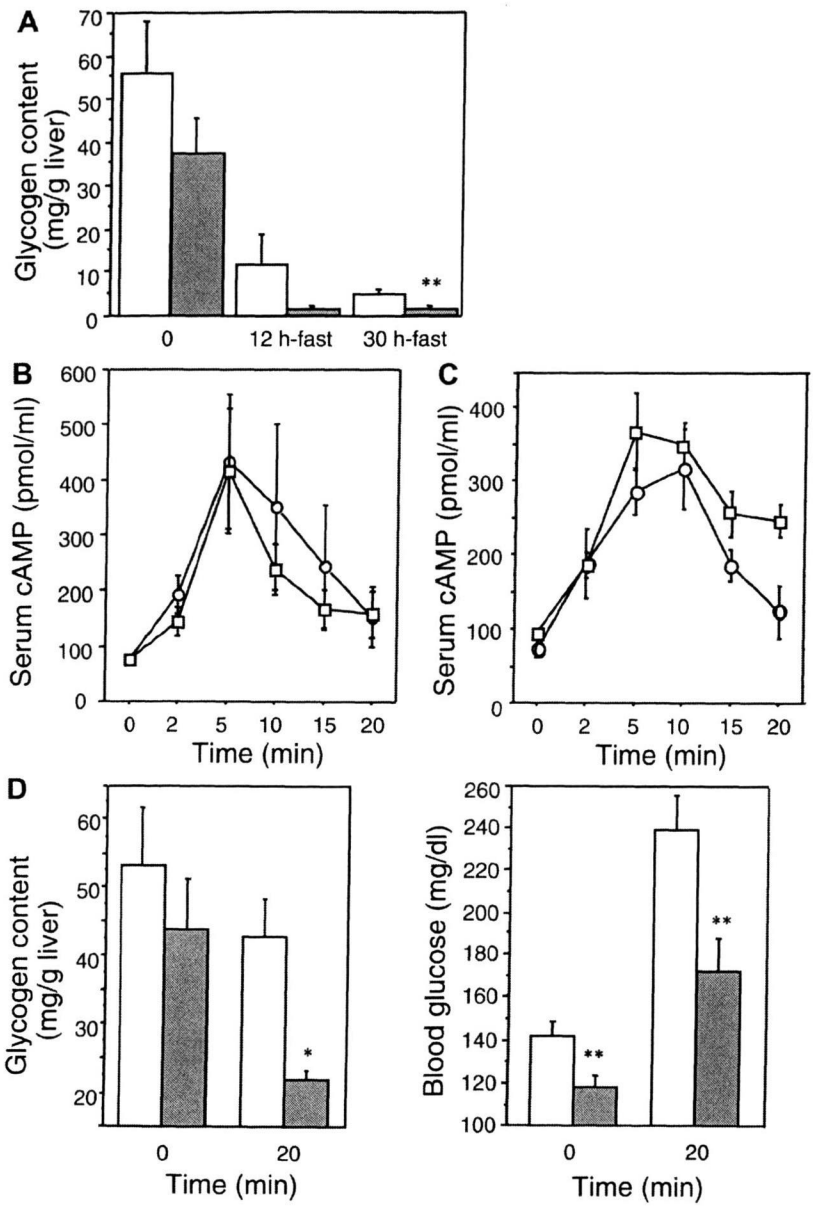

Fig. 8. Glycogenolysis in the liver. *A*: changes in hepatic glycogen content during fasting. Glycogen content in liver was measured before and after 12 and 30 h of fasting. Values are means ± SE obtained from analysis of WT (open bars; $n = 6$) and $p85\alpha^{-/-}$ mice (filled bars; $n = 6$). $^{**}P < 0.01$ compared with WT mice. *B*: changes in the plasma cAMP level after glucagon stimulation. Freely fed mice were given 0.05 U of human glucagon per kg of body weight. Plasma cAMP levels were then measured at the indicated time points. Values are means ± SE obtained from the analysis of WT (○; $n = 8$) and $p85\alpha^{-/-}$ mice (□; $n = 12$). *C*: changes in plasma cAMP level after isoproterenol stimulation. Freely fed mice were given 0.5 μg of human isoproterenol. Plasma cAMP levels were then measured at the indicated time points. Values are means ± SE obtained from the analysis of WT (○; $n = 6$) and $p85\alpha^{-/-}$ mice (□; $n = 6$). *D*: changes in hepatic glycogen content and plasma glucose levels in response to glucagon. Fed mice were given 0.05 U of human glucagon per kg of body weight. Hepatic glycogen contents (*left*) and plasma glucose levels (*right*) were measured at indicated time points. Values are means ± SE obtained from the analysis of WT (open bars; $n = 8$) and $p85\alpha^{-/-}$ mice (filled bars; $n = 8$). $^{*}P < 0.05$, $^{**}P < 0.01$ compared with WT mice.

not affected by the lack of $p85\alpha$ in the liver. The absence of improvement in insulin-stimulated PI3K activation in the liver of $p85\alpha$-deficient mice, unlike the muscles, may be associated with the molecular balance between the regulatory subunit and the catalytic subunit of PI3K. In $p85\alpha$-deficient mice, glucose production from the liver was rather elevated, but not suppressed, in marked contrast to the increased insulin sensitivity in peripheral tissues. Consequently, the liver seemed to partially compensate for the increase in glucose uptake in peripheral tissues in $p85\alpha$-deficient mice.

ACKNOWLEDGMENTS

We thank Eri Yoshida-Nagata, Yuko Muto, Hiroshi Chiyonobu, Eri Sakamoto, and Mitsuyo Kaji for excellent technical assistance and animal care.

GRANTS

This work was supported by a grant for Life & Socio-Medical Science from the Kanae Foundation, a Grant-in-aid from the Mochida Memorial Foundation for Medical and Pharmaceutical Research (to Y. Terauchi), a Grant-in-aid for Scientific Research (C) 19591062 from the Ministry of Education, Culture, Sports, Science and Technology of Japan (to K. Aoki); a Grant-in-Aid for Creative Scientific Research (10NP0201) from the Japan Society for the Promotion of Science; and a Grant-in-Aid for the Development of Innovative Technology from the Ministry of Education, Culture, Sports, Science and Technology of Japan, Health Science Research Grants (Research on the Human Genome and Gene Therapy) from the Ministry of Health and Welfare (to T. Kadowaki). This work was also supported by the Yokohama City University Center of Excellence Program of the Ministry of Education, Culture, Sports, Science and Technology of Japan and a grant for the Strategic Research Project of Yokohama City University (K18005; to Y. Terauchi).

REFERENCES

1. **Agati JM, Yeagley D, Quinn PG.** Assessment of the roles of mitogen-activated protein kinase, phosphatidylinositol 3-kinase, protein kinase B, and protein kinase C in insulin inhibition of cAMP-induced phosphoenolpyruvate carboxykinase gene transcription. *J Biol Chem* 273: 18751–18759, 1998.
2. **Antonetti DA, Algenstaedt P, Kahn CR.** Insulin receptor substrate 1 binds two novel splice variants of the regulatory subunit of phosphatidylinositol 3-kinase in muscle and brain. *Mol Cell Biol* 16: 2195–2203, 1996.
3. **Aoki K, Taniguchi H, Ito Y, Satoh S, Nakamura S, Muramatsu K, Yamashita R, Ito S, Mori Y, Sekihara H.** Dehydroepiandrosterone decreases elevated hepatic glucose production in C57BL/KsJ-db/db mice. *Life Sci* 74: 3075–3084, 2004.
4. **Bergmeyer J, Graszl M.** *Methods of Enzymatic Analysis* (3rd ed.). Weinheim, Germany: Verlag Chimie, 1984, vo. VI, pp. 185–198, 342–250, 555–561.
5. **Chen D, Mauvais-Jarvis F, Bluher M, Fisher SJ, Jozsi A, Goodyear LJ, Ueki K, Kahn CR.** p50alpha/p55alpha phosphoinositide 3-kinase knockout mice exhibit enhanced insulin sensitivity. *Mol Cell Biol* 24: 320–329, 2004.
6. **Dea MK, Van Citters GW, Ader M, Mittelman SD, Sunehag AL, Bergman RN.** Paradoxical effect of troglitazone in normal animals: enhancement of adipocyte but reduction of liver insulin sensitivity. *Diabetes* 49: 2087–2093, 2000.
7. **Dickens M, Svitek CA, Culbert AA, O'Brien RM, Tavaré JM.** Central role for phosphatidylinositide 3-kinase in the repression of glucose-6-phosphatase gene transcription by insulin. *J Biol Chem* 273: 20144–20149, 1998.
8. **Fruman DA, Cantley LC, Carpenter CL.** Structural organization and alternative splicing of the murine phosphoinositide 3-kinase p85 alpha gene. *Genomics* 37: 113–121, 1996.
9. **Fruman DA, Snapper SB, Yballe CM, Davidson L, Yu JY, Alt FW, Cantley LC.** Impaired B cell development and proliferation in absence of phosphoinositide 3-kinase p85alpha. *Science* 283: 393–397, 1999.
10. **Fujiwara T, Okuno A, Yoshioka S, Horikoshi H.** Suppression of hepatic gluconeogenesis in long-term troglitazone treated diabetic KK and C57BL/KsJ-db/db mice. *Metabolism* 44: 486–490, 1995.
11. **Fukao T, Tanabe M, Terauchi Y, Ota T, Matsuda S, Asano T, Kadowaki T, Takeuchi T, Koyasu S.** PI3K-mediated negative feedback regulation of IL-12 production in DCs. *Nat Immunol* 3: 875–881, 2002.
12. **Geering B, Cutillas PR, Nock G, Gharbi SI, Vanhaesebroeck B.** Class 1A phosphoinositide 3-kinases are obligate p85-p110 heterodimers. *Proc Natl Acad Sci USA* 104: 7809–7814, 2007.
13. **Holman GD, Kasuga M.** From receptor to transporter: insulin signalling to glucose transport. *Diabetologia* 40: 991–1003, 1997.
14. **Imai J, Katagiri H, Yamada T, Ishigaki Y, Suzuki T, Kudo H, Uno K, Hasegawa Y, Gao J, Kaneko K, Ishihara H, Niijima A, Nakazato M, Asano T, Minokoshi Y, Oka Y.** Regulation of pancreatic beta cell mass by neuronal signals from the liver. *Science* 322: 1250–1254, 2008.
15. **Inukai K, Anai M, Van Breda E, Hosaka T, Katagiri H, Funaki M, Fukushima Y, Ogihara T, Yazaki Y, Kikuchi Oka Y, Asano T.** A novel 55-kDa regulatory subunit for phosphatidylinositol 3-kinase structurally similar to p55PIK Is generated by alternative splicing of the p85alpha gene. *J Biol Chem* 271: 5317–5320, 1996.
16. **Inukai K, Funaki M, Ogihara T, Katagiri H, Kanda A, Anai M, Fukushima Y, Hosaka T, Suzuki M, Shin BC, Takata K, Yazaki Y, Kikuchi M, Oka Y, Asano T.** p85alpha gene generates three isoforms of regulatory subunit for phosphatidylinositol 3-kinase (PI 3-kinase), p50alpha, p55alpha, and p85alpha, with different PI 3-kinase activity elevating responses to insulin. *J Biol Chem* 272: 7873–7882, 1997.
17. **Kadowaki T, Tobe K, Honda-Yamamoto R, Tamemoto H, Kaburagi Y, Momomura K, Ueki K, Takahashi Y, Yamauchi T, Akanuma Y, Yazaki Y.** Signal transduction mechanism of insulin and insulin-like growth factor-1. *Endocr J* 43: 33–41, 1996.
18. **Knight ZA, Gonzalez B, Feldman ME, Zunder ER, Goldenberg DD, Williams O, Loewith R, Stokoe D, Balla A, Toth B, Balla T, Weiss WA, Williams RL, Shokat KM.** A pharmacological map of the PI3-K family defines a role for p110alpha in insulin signaling. *Cell* 19: 733–747, 2006.
19. **Kubota N, Kubota T, Itoh S, Kumagai H, Kozono H, Takamoto I, Mineyama T, Ogata H, Tokuyama K, Ohsugi M, Sasako T, Moroi M, Sugi K, Kakuta S, Iwakura Y, Noda T, Ohnishi S, Nagai R, Tobe K, Terauchi Y, Ueki K, Kadowaki T.** Dynamic functional relay between insulin receptor substrate 1 and 2 in hepatic insulin signaling during fasting and feeding. *Cell Metab* 8: 49–64, 2008.
20. **Kubota N, Terauchi Y, Kubota T, Kumagai H, Itoh S, Satoh H, Yano W, Ogata H, Tokuyama K, Takamoto I, Mineyama T, Ishikawa M, Moroi M, Sugi K, Yamauchi T, Ueki K, Tobe K, Noda T, Nagai R, Kadowaki T.** Pioglitazone ameliorates insulin resistance and diabetes by both adiponectin-dependent and -independent pathways. *J Biol Chem* 281: 8748–8755, 2006.
21. **Kubota N, Terauchi Y, Tobe K, Yano W, Suzuki R, Ueki K, Takamoto I, Satoh H, Maki T, Kubota T, Moroi M, Okada-Iwabu M, Ezaki O, Nagai R, Ueta Y, Kadowaki T, Noda T.** Insulin receptor substrate 2 plays a crucial role in beta cells and the hypothalamus. *J Clin Invest* 114: 917–927, 2004.
22. **Kubota N, Tobe K, Terauchi Y, Eto K, Yamauchi T, Suzuki R, Tsubamoto Y, Komeda K, Nakano R, Miki H, Satoh S, Sekihara H, Sciacchitano S, Lesniak M, Aizawa S, Nagai R, Kimura S, Akanuma Y, Taylor SI, Kadowaki T.** Disruption of insulin receptor substrate 2 causes type 2 diabetes because of liver insulin resistance and lack of compensatory beta-cell hyperplasia. *Diabetes* 49: 1880–1889, 2000.
23. **Kubota N, Yano W, Kubota T, Yamauchi T, Itoh S, Kumagai H, Kozono H, Takamoto I, Okamoto S, Shiuchi T, Suzuki R, Satoh H, Tsuchida A, Moroi M, Sugi K, Noda T, Ebinuma H, Ueta Y, Kondo T, Araki E, Ezaki O, Nagai R, Tobe K, Terauchi Y, Ueki K, Minokoshi Y, Kadowaki T.** Adiponectin stimulates AMP-activated protein kinase in the hypothalamus and increases food intake. *Cell Metab* 6: 55–68, 2007.
24. **Lavan BE, Lane WS, Lienhard GE.** The 60-kDa phosphotyrosine protein in insulin-treated adipocytes is a new member of the insulin receptor substrate family. *J Biol Chem* 272: 11439–11443, 1997.
25. **Mauvais-Jarvis F, Ueki K, Fruman DA, Hirshman MF, Sakamoto K, Goodyear LJ, Iannacone M, Accili D, Cantley LC, Kahn CR.** Reduced expression of the murine p85alpha subunit of phosphoinositide 3-kinase improves insulin signaling and ameliorates diabetes. *J Clin Invest* 109: 141–149, 2002.
26. **Mithieux G, Daniele N, Payrastre B, Zitoun C.** Liver microsomal glucose-6-phosphatase is competitively inhibited by the lipid products of phosphatidylinositol 3-kinase. *J Biol Chem* 273: 17–19, 1998.
27. **Moore MC, Connolly CC, Cherrington AD.** Autoregulation of hepatic glucose production. *Eur J Endocrinol* 138: 240–248, 2000.
28. **O'Brien RM, Granner JM.** *Gene Regulation in Diabetes Mellitus.* Philadelphia, PA: Lippincott-Raven, edited by DK LeRoith, D, Taylor, and SI Olefsky. 2000, pp. 291–304.
29. **Okkenhaug K, Vanhaesebroeck B.** New responsibilities for the PI3K regulatory subunit p85 alpha. *Sci STKE* 16: PE1, 2001.
30. **Plum L, Schubert M, Brüning JC.** The role of insulin receptor signaling in the brain. *Trends Endocrinol Metab* 16: 59–65, 2005.
31. **Rous S.** Effect of insulin on incorporation of ^{14}C-labeled pyruvates and bicarbonate into blood glucose of fasted mice. *Am J Physiol Endocrinol Metab* 235: E22–E26, 1978.
32. **Summers SA, Yin VP, Whiteman EL, Garza LA, Cho H, Tuttle RL, Birnbaum MJ.** Signaling pathways mediating insulin-stimulated glucose transport. *Ann NY Acad Sci* 892: 169–186, 1999.
33. **Sun XJ, Rothenberg P, Kahn CR, Backer JM, Araki E, Wilden PA, Cahill DA, Goldstein BJ, White MF.** Structure of the insulin receptor substrate IRS-1 defines a unique signal transduction protein. *Nature* 352: 73–77, 1991.
34. **Sun XJ, Wang LM, Zhang Y, Yenush L, Myers MG Jr, Glasheen E, Lane WS, Pierce JH, White MF.** Role of IRS-2 in insulin and cytokine signalling. *Nature* 377: 173–177, 1995.
35. **Sutherland C, O'Brien RM, Granner DK.** Phosphatidylinositol 3-kinase, but not p70/p85 ribosomal S6 protein kinase, is required for the regulation of phosphoenolpyruvate carboxykinase (PEPCK) gene expression by insulin. Dissociation of signaling pathways for insulin and phorbol ester regulation of PEPCK gene expression. *J Biol Chem* 270: 15501–15506, 1995.
36. **Suzuki R, Tobe K, Aoyama M, Inoue A, Sakamoto K, Yamauchi T, Kamon J, Kubota N, Terauchi Y, Yoshimatsu H, Matsuhisa M, Nagasaka S, Ogata H, Tokuyama K, Nagai R, Kadowaki T.** Both insulin signaling defects in the liver and obesity contribute to insulin resistance and cause diabetes in Irs2(−/−) mice. *J Biol Chem* 279: 25039–25049, 2004.
37. **Taniguchi CM, Kondo T, Sajan M, Luo J, Bronson R, Asano T, Farese R, Cantley LC, Kahn CR.** Divergent regulation of hepatic glucose and lipid metabolism by phosphoinositide 3-kinase via Akt and PKClambda/zeta. *Cell Metab* 3: 343–353, 2006.

38. **Taniguchi CM, Tran TT, Kondo T, Luo J, Ueki K, Cantley LC, Kahn CR.** Phosphoinositide 3-kinase regulatory subunit p85alpha suppresses insulin action via positive regulation of PTEN. *Proc Natl Acad Sci USA* 103: 12093–12097, 2006.
39. **Taylor SI.** Deconstructing type 2 diabetes. *Cell* 97: 9–12, 1999.
40. **Terauchi Y, Iwamoto K, Tamemoto H, Komeda K, Ishii C, Kanazawa Y, Asanuma N, Aizawa T, Akanuma Y, Yasuda K, Kodama T, Tobe K, Yazaki Y, Kadowaki T.** Development of non-insulin-dependent diabetes mellitus in the double knockout mice with disruption of insulin receptor substrate-1 and beta cell glucokinase genes. Genetic reconstitution of diabetes as a polygenic disease. *J Clin Invest* 99: 861–866, 1997.
41. **Terauchi Y, Matsui J, Kamon J, Yamauchi T, Kubota N, Komeda K, Aizawa S, Akanuma Y, Tomita M, Kadowaki T.** Increased serum leptin protects from adiposity despite the increased glucose uptake in white adipose tissue in mice lacking p85alpha phosphoinositide 3-kinase. *Diabetes* 53: 2261–2270, 2004.
42. **Terauchi Y, Takamoto I, Kubota N, Matsui J, Suzuki R, Komeda K, Hara A, Toyoda Y, Miwa I, Aizawa S, Tsutsumi S, Tsubamoto Y, Hashimoto S, Eto K, Nakamura A, Noda M, Tobe K, Aburatani H, Nagai R, Kadowaki T.** Glucokinase and IRS-2 are required for compensatory beta cell hyperplasia in response to high-fat diet-induced insulin resistance. *J Clin Invest* 117: 246–257, 2007.
43. **Terauchi Y, Tsuji Y, Satoh S, Minoura H, Murakami K, Okuno A, Inukai K, Asano T, Kaburagi Y, Ueki K, Nakajima H, Hanafusa T, Matsuzawa Y, Sekihara H, Yin Y, Barrett JC, Oda H, Ishikawa T, Akanuma Y, Komuro I, Suzuki M, Yamamura K, Kodama T, Suzuki H, Yamamura K, Kodama T, Suzuki H, Koyasu S, Aizawa S, Tobe K, Fukui Y, Yazaki Y, Kadowaki T.** Increased insulin sensitivity and hypoglycaemia in mice lacking the p85 alpha subunit of phosphoinositide 3-kinase. *Nat Genet* 21: 230–235, 1999.
44. **Ueki K, Algenstaedt P, Mauvais-Jarvis F, Kahn CR.** Positive and negative regulation of phosphoinositide 3-kinase-dependent signaling pathways by three different gene products of the p85alpha regulatory subunit. *Mol Cell Biol* 20: 8035–8046, 2000.
45. **Ueki K, Fruman DA, Brachmann SM, Tseng YH, Cantley LC, Kahn CR.** Molecular balance between the regulatory and catalytic subunits of phosphoinositide 3-kinase regulates cell signaling and survival. *Mol Cell Biol* 22: 965–977, 2002.
46. **Uno K, Katagiri H, Yamada T, Ishigaki Y, Ogihara T, Imai J, Hasegawa Y, Gao J, Kaneko K, Iwasaki H, Ishihara H, Sasano H, Inukai K, Mizuguchi H, Asano T, Shiota M, Nakazato M, Oka Y.** Neuronal pathway from the liver modulates energy expenditure and systemic insulin sensitivity. *Science* 312: 1656–1659, 2006.
47. **Withers DJ, White M.** Perspective: the insulin signaling system–a common link in the pathogenesis of type 2 diabetes. *Endocrinology* 141: 1917–1921, 2000.
48. **Yamauchi T, Tobe K, Tamemoto H, Ueki K, Kaburagi Y, Yamamoto-Honda R, Takahashi Y, Yoshizawa F, Aizawa S, Akanuma Y, Sonenberg N, Yazaki Y, Kadowaki T.** Insulin signalling and insulin actions in the muscles and livers of insulin-resistant, insulin receptor substrate 1-deficient mice. *Mol Cell Biol* 16: 3074–3084, 1996.

THE JOURNAL OF BIOLOGICAL CHEMISTRY VOL. 284, NO. 10, pp. 6061–6070, March 6, 2009

Growth Hormone Inhibition of Glucose Uptake in Adipocytes Occurs without Affecting GLUT4 Translocation through an Insulin Receptor Substrate-2-Phosphatidylinositol 3-Kinase-dependent Pathway*

Received for publication, October 29, 2008, and in revised form, December 15, 2008 Published, JBC Papers in Press, January 2, 2009, DOI 10.1074/jbc.M808282200

Naoko Sasaki-Suzuki[‡§1], Kiyoshi Arai[‡2], Tomomi Ogata[‡3], Kouhei Kasahara[‡], Hideyuki Sakoda[¶], Kazuhiro Chida[‡], Tomoichiro Asano[¶‖], Jeffrey E. Pessin[§], Fumihiko Hakuno[‡], and Shin-Ichiro Takahashi[‡4]**

*From the [‡]Departments of Animal Sciences and Applied Biological Chemistry, Graduate School of Agriculture and Life Sciences, University of Tokyo, 1-1-1 Yayoi, Bunkyo-ku, Tokyo 113-8657, Japan, the [§]Department of Pharmacological Sciences, State University of New York, Stony Brook, New York 11794, the [¶]Department of Internal Medicine, Graduate School of Medicine, University of Tokyo, 7-3-1 Hongo, Bunkyo-ku, Tokyo 113-8655, Japan, the [‖]Division of Molecular Medical Science, Graduate School of Biomedical Sciences, Hiroshima University, Minami-ku, Hiroshima 734-8553, Japan, and the **Departments of Medicine and Molecular Pharmacology, Albert Einstein College of Medicine, Bronx, New York 10461*

Growth hormone (GH) pretreatment of 3T3-L1 adipocytes resulted in a concentration- and time-dependent inhibition of insulin-stimulated glucose uptake. Surprisingly, this occurred without significant effect on insulin-stimulated glucose transporter (GLUT) 4 translocation or fusion with the plasma membrane. In parallel, the inhibitory actions of chronic GH pretreatment also impaired insulin-dependent activation of phosphatidylinositol (PI) 3-kinase bound to insulin receptor substrate (IRS)-2 but not to IRS-1. In addition, insulin-stimulated Akt phosphorylation was inhibited by GH pretreatment. In contrast, overexpression of IRS-2 or expression of a constitutively active Akt mutant prevented the GH-induced insulin resistance of glucose uptake. Moreover, small interfering RNA-mediated IRS-2 knockdown also inhibited insulin-stimulated Akt activation and glucose uptake without affecting GLUT4 translocation and plasma membrane fusion. Together, these data support a model in which chronic GH stimulation inhibits insulin-dependent activation of phosphatidylinositol 3-kinase through a specific interaction of phosphatidylinositol 3-kinase bound to IRS-2. This inhibition leads to suppression of Akt activation coupled to glucose transport activity but not translocation or plasma membrane fusion of GLUT4.

Insulin is the major anabolic hormone whose action plays pivotal roles in tissue development, growth, and the maintenance of glucose homeostasis. Insulin regulates glucose metabolism at several levels, reducing hepatic glucose production and increasing the rate of glucose uptake into skeletal muscle and adipose tissue. Insulin-responsive glucose transporter isoform GLUT4[5] is expressed in skeletal muscle and adipose tissue and is known to be responsible for the glucose uptake into these tissues (1–3). Thus, glucose uptake through GLUT4 plays a central role in the regulation of postprandial glucose clearance from the plasma. Dysfunction in the ability of insulin to stimulate glucose uptake results in states of insulin resistance that plays a major role in the development of type 2 diabetes mellitus.

Insulin binding to the extracellular domain of the insulin receptor on the plasma membrane of target cells activates its intrinsic cytoplasmic tyrosine kinase activity (4, 5). The activated insulin receptor tyrosine kinase phosphorylates a variety of substrates, including insulin receptor substrates (IRSs) and Shc (6, 7). Tyrosine phosphorylation of these substrates leads to their binding to several Src homology 2 domain-containing signaling molecules, including p85 PI 3-kinase regulatory subunit and Grb2 (6, 8). This binding resulted in activation of distinct signaling cascades, for example Ras- mitogen-activated protein kinase (MAPK) and PI 3-kinase cascades (7, 9). It is well known that these two pathways are directly linked to specific downstream biological responses that account for several of the known actions of insulin. In particular, the PI 3-kinase-depend-

* This work was supported, in whole or in part, by a National Institutes of Health grant (to J. E. P.). This work was also supported by a grant-in-aid for international joint research (to S.-I. T.) from Japan Society for the Promotion of Science, Grants-in-aid for Scientific Research (B)(2) 11460126, Exploratory Research 15658080, and Scientific Research (A)(2) 16208028) from the Ministry of Education, Science and Culture of Japan (to S.-I. T.), and by the Program for Promotion of Basic Research Activities for Innovative Biosciences (to F. H.). The costs of publication of this article were defrayed in part by the payment of page charges. This article must therefore be hereby marked "*advertisement*" in accordance with 18 U.S.C. Section 1734 solely to indicate this fact.

[1] Present address: Iwanaga Writers' Club LLC., 15-3 Sakuragaoka-cho, Shibuya-ku, Tokyo 150-0031, Japan.

[2] Present address: Group I, Biological Research Laboratories I, R & D Division, Daiichi-Sankyo Co., Ltd., Shinagawa R & D Center, 1-2-58 Hiromachi, Shinagawa-ku, Tokyo, 140-8710, Japan.

[3] Present address: Metabolic Disorders 1, Discovery Research Laboratories, Kyorin Pharmaceutical Co., Ltd., 2399-1 Nogi, Nogi-machi, Shimotsuga-gun, Tochigi 329-0114, Japan.

[4] To whom correspondence should be addressed: Graduate School of Agriculture and Life Sciences, University of Tokyo, 1-1-1 Yayoi, Bunkyo-ku, Tokyo 113-8657, Japan. Tel.: 81-3-5841-1310; Fax: 81-3-5841-1311; E-mail: atkshin@mail.ecc.u-tokyo.ac.jp.

[5] The abbreviations used are: GLUT, glucose transporter; GH, growth hormone; PI, phosphatidylinositol; IRS, insulin receptor substrate; PIP_3, phosphoinositide 3,4,5-triphosphate; PDK, phosphoinositide-dependent kinase; DMEM, Dulbecco's modified Eagle's medium; PBS, phosphate-buffered saline; FBS, fetal bovine serum; NC, nonrelevant control; GFP, green fluorescent protein; PI, phosphatidylinositol; siRNA, small interfering RNA.

ent pathway is a well established requirement for insulin-induced glucose uptake in adipose and muscle tissue (10–16).

Activated PI 3-kinase phosphorylates phosphatidylinositol and generates phosphoinositide 3,4,5-triphosphate (PIP_3). PIP_3 production recruits Akt kinase to the plasma membrane, where Akt is phosphorylated by phosphoinositide-dependent kinases, resulting in activation of the Akt kinase (17). Activated Akt phosphorylates various Akt substrates, including AS160, GTPase-activating protein for Rab10 (18). Recently, it was reported that phosphorylation and inhibition of AS160 and subsequent activation of small GTP-binding protein Rab10 are sufficient for GLUT4 translocation to plasma membrane (19).

Growth hormone (GH) is well known to possess bioactivities regulating both growth and metabolism. In various tissues, GH is known to mediate anti-insulin effects on glucose and lipid metabolism. Insulin resistance is often observed in acromegalic patients, and GH administration to GH-deficient patients has been observed to increase the incidence of diabetes mellitus (20–22). Recently, we have reported that the GH transgenic rat, in which human GH was highly expressed, showed an insulin-resistant phenotype in both muscle and adipose tissues (23). Similarly, chronic GH treatment in cultured 3T3-L1 adipocytes was also found to impair insulin-induced glucose uptake (24). Together, these studies indicate that chronic GH treatment can result in insulin-resistant glucose uptake *in vitro* as well as *in vivo*.

Thus, this study was undertaken to evaluate the molecular mechanism of GH-induced impairment of insulin-dependent glucose uptake in 3T3-L1 adipocytes. Here we showed that chronic GH pretreatment inhibits insulin-induced glucose uptake without affecting GLUT4 translocation, through the reduction of IRS-2-associated PI 3-kinase activity.

EXPERIMENTAL PROCEDURES

Materials—Dulbecco's modified Eagle's medium (DMEM), phosphate-buffered saline (PBS), and Hanks' buffered salt solution were purchased from Nissui (Tokyo, Japan). Calf serum and fetal bovine serum (FBS) were obtained from JRH Bioscience (Tokyo, Japan). Penicillin and streptomycin were obtained from Ban'yu Pharmaceutical Co. (Tokyo, Japan). Recombinant human GH was kindly donated from Dainippon Sumitomo Pharmaceutical Co., Ltd. (Osaka, Japan), and CR Pharmaceuticals Co., Ltd. (Kobe, Japan). Bovine insulin was obtained from Sigma. Anti-IRS-1 antibody and anti-IRS-2 antibody were raised in rabbits as described previously (25). Anti-JAK2 antibody, anti-GLUT1 antibody, anti-GLUT4 antibody, and anti-IRβ antibody were obtained from Santa Cruz Biotechnology. Anti-PI 3-kinase p85 antibody and anti-c-Myc antibody were obtained from Upstate Biotechnology, Inc. (Lake Placid, NY). Anti-phospho-Akt (Ser-473) antibody and anti-Akt antibody were obtained from Cell Signaling Technology, Inc. (Beverly, MA). Anti-phospho-Akt (Thr-308) antibody, anti-β-actin antibody, and anti-phosphotyrosine antibody were obtained from Sigma. Texas Red dye-conjugated anti-mouse IgG was obtained from Jackson ImmunoResearch (West Grove, PA). Protein A-Sepharose and 2-deoxy-D-[2,6-^{3}H]glucose (1 mCi/ml) were purchased from Amersham Biosciences. Wheat germ agglutinin-agarose was obtained from Seikagaku Co. (Tokyo, Japan). Random control, IRS-1-, and IRS-2-specific siRNAs were purchased from RNAi Corp. (Tokyo, Japan). The sequence of the IRS-1 siRNA used was CUC GAG AGC UGU UUC AAC AUC. The sequence of the IRS-2 siRNA used was GCC CGA ACC UCA AUA ACA ACA. The control siRNA sequence was GUA CCG CAC GUC AUU CGU AUC. Other chemicals were of reagent grade available commercially.

Cell Culture of 3T3-L1 Adipocytes—Murine 3T3-L1 preadipocytes were purchased from the American Type Tissue Culture repository. 3T3-L1 preadipocytes were maintained at 37 °C in a humidified 5% CO_2 controlled atmosphere in DMEM supplemented with 10% calf serum, 50 IU/ml penicillin, 50 μg/ml streptomycin, 0.5 μg/ml amphotericin B (Sankyo, Tokyo, Japan). 3T3-L1 preadipocytes were induced to differentiate into adipocytes as described previously (27). Briefly, confluent cultures were incubated with DMEM containing 10% FBS, 1 μg/ml insulin, 1 mM dexamethasone, and 0.5 mM isobutyl-1-methylxanthine. After 4 days, the medium was changed to DMEM containing 10% FBS and 1 μg/ml insulin for an additional 2 days. The medium was then changed to DMEM containing 10% FBS. Cells were used for experiments at 6–10 days after inducing differentiation, when more than 90% of cells displayed an adipocyte phenotype.

Electroporation of 3T3-L1 Adipocytes—Transient transfection of 3T3-L1 adipocytes was described previously (26). Briefly, fully differentiated 3T3-L1 adipocytes were detached from the tissue culture plates by trypsin buffer (0.25% trypsin, 0.02% EDTA in PBS) and electroporated with a total of 100 μg of plasmid or 1 nmol of siRNA using the Gene Pulser II (Bio-Rad) at 0.15 kV and 0.95 microfarad.

Measurement of Glucose Uptake—3T3-L1 adipocytes were incubated with the indicated concentrations of insulin in Krebs-Ringer phosphate buffer for 15 min at 37 °C. Then 0.1 mM 2-deoxy-D-glucose containing 10 μCi/ml 2-deoxy-D-[2,6-^{3}H]glucose was added, and cells were incubated for 10 min at 37 °C. The reaction was terminated by addition of ice-cold PBS containing 10 mM D-glucose. Cells were lysed with 0.05 N NaOH containing 0.1% SDS, and radioactivity taken up by the cells was measured by liquid scintillation counter.

Subcellular Fractionation—3T3-L1 adipocytes were scraped and homogenized in HES buffer (20 mM Tris-HCl, pH 7.4, 255 mM sucrose, 1 mM EDTA) with 20 strokes using a Dounce homogenizer. Homogenates were centrifuged at 16,000 × *g* for 15 min. The resulting pellet obtained from this spin was layered onto 1.12 M sucrose in HES buffer and centrifuged at 101,000 × *g* for 70 min. This yielded a white fluffy band at the interface, plasma membrane fraction. The plasma membrane fraction was resuspended in HES buffer and pelleted at 48,000 × *g* for 20 min. The resulting pellets were resuspended in Tris/Triton lysis buffer (50 mM Tris-HCl, pH 8.0, 150 mM NaCl, 1 mM NaF, 1 mM EDTA, 1 mM EGTA, 1.5 mM $MgCl_2$, 10% glycerol, 1% Triton X-100, 10 μg/ml leupeptin, 5 μg/ml pepstatin, 20 μg/ml phenylmethylsulfonyl fluoride, 100 kallikrein-inactivating units/ml aprotinin, 0.5 mM Na_3VO_4, and 10 mg/ml *p*-nitrophenyl phosphate).

Biotinylation of Cell Surface Protein and Isolation of Biotinylated Protein—3T3-L1 adipocytes pretreated with or without GH were stimulated with insulin. Cells were washed with ice-cold PBS and incubated with 0.5 mg/ml NHS-LC (succinimidyl-6-[biotinamido]hexanoate) biotin (Pierce) in PBS for 30 min at 4 °C. The reaction was stopped by rinsing the plates three times with 15 mM glycine in ice-cold PBS. The cells were then collected and solubilized with Tris/Triton lysis buffer. For isolating biotinylated protein, whole cell lysates were mixed with streptavidin-agarose beads (Sigma), and the suspension was incubated at 4 °C overnight. The streptavidin-agarose beads were spun down and washed three times with lysis buffer, once with NaCl buffer (50 mM Tris-HCl, pH 8.0, 1 M NaCl, 1 mM NaF, 1 mM EDTA, 1 mM EGTA, 1.5 mM $MgCl_2$, 10% glycerol, 1% Triton X-100), once with 10% Tris/Triton lysis buffer in distilled water, and once with lysis buffer containing 0.1% in SDS. The pellet as biotinylated protein and supernatant as nonbiotinylated protein were collected (28–30).

Immunofluorescence and GLUT4-myc-GFP Translocation Assay—3T3-L1 adipocytes were electroporated with or without siRNA along with pGlut4-myc-green fluorescent protein (GFP). Two days after electroporation, cells were serum-starved for 2 h and treated with or without 100 nM GH followed by insulin treatment. Cells were fixed without permeabilization and immunostained with anti-Myc antibody. Cells were imaged using confocal fluorescence microscopy (OLYMPUS, Tokyo, Japan). To detect GLUT4 translocation to the cell surface, we quantified the ratio of Myc-rimed cells to GFP-transfected cells.

Analyses of Insulin Signals—3T3-L1 adipocytes were serum-starved for 2 h in DMEM containing 0.1% bovine serum albumin. Cells were treated with or without 100 nM GH followed by treatment with 0.1 nM insulin. Cells were harvested by Tris/Triton lysis buffer. After centrifugation of the homogenates at 12,000 × *g* for 10 min at 4 °C, supernatant was collected as whole cell lysates. The whole cell lysates were subjected to protein assay using protein assay kit (Bio-Rad). One mg of whole cell lysates was used for immunoprecipitation with indicated antibodies. Precipitants were separated by SDS-PAGE and then immunoblotted with the indicated antibodies.

PI 3-Kinase Activity Assay—PI 3-kinase activity assay was carried out as described before (31). Briefly, 3T3-L1 adipocytes were serum-starved for 2 h in DMEM containing 0.1% bovine serum albumin followed by pretreatment with or without 100 nM GH for 24 h. Cells were treated with or without 0.1 nM insulin for 10 min. Cells were lysed by Tris/Nonidet P-40 lysis buffer (50 mM Tris-HCl, pH 8.0, 150 mM NaCl, 1 mM NaF, 1 mM EDTA, 1 mM EGTA, 1.5 mM $MgCl_2$, 10% glycerol, 1% Nonidet P-40, 10 μg/ml leupeptin, 5 μg/ml pepstatin, 20 μg/ml phenylmethylsulfonyl fluoride, 100 kallikrein-inactivating units/ml aprotinin, 0.5 mM Na_3VO_4, and 10 mg/ml *p*-nitrophenyl phosphate). One mg of whole cell lysates was immunoprecipitated with anti-IRS-1 antibody or anti-IRS-2 antibody. Immunoprecipitates were washed once with Tris/Nonidet P-40 buffer, LiCl buffer (100 mM Tris-HCl, pH 7.5, and 500 mM LiCl), distilled water, and TNE buffer (10 mM Tris-HCl, pH 7.5, 150 mM NaCl, and 1 mM EDTA) and finally resuspended in 40 μl of reaction buffer (20 mM Tris-HCl, pH 7.5, 100 mM NaCl, and 0.5 mM EGTA). Kinase reaction was initiated by incubation of immunocomplex in reaction buffer with 20 mM [γ-^{32}P]ATP (4 μCi/mmol), 20 mM $MgCl_2$, and 0.5 μg/μl phosphatidylinositol at 25 °C for 25 min. Reaction was stopped by adding chloroform/methanol/HCl (10:20:1). A lipid product was extracted, spotted onto silica gel plate, and developed with chloroform/methanol/NH_4OH/water (43:38:6:6). ^{32}P radioactivity incorporated into phosphatidylinositol was measured by autoradiography as PI 3-kinase activity.

Adenovirus Preparation and Infection to 3T3-L1 Cells—The recombinant adenoviruses, Ade-myr-Akt (constitutive active form of Akt) and Ade-LacZ (LacZ) were prepared described before (32). The recombinant adenovirus to express IRS-2 was constructed as described before (33). Adenoviruses were amplified in human embryonic kidney 293 cells. 3T3-L1 adipocytes were infected with adenovirus by incubating cells with 100 multiplicities of infection of adenovirus. Cells were used for experiments after 48 h of infection.

Statistical Analysis—Statistical analyses of data were performed by two-way or three-way analysis of variance followed by Fisher's PSLD post-hoc test using StatView software (Abacus Concepts, Inc., Berkeley, CA). The results shown are the mean ± S.E. $p < 0.05$ was considered statistically significant.

RESULTS

Chronic GH Pretreatment Inhibits Insulin-stimulated Glucose Uptake in 3T3-L1 Adipocytes—It has been reported that chronic GH pretreatment inhibits insulin-dependent glucose uptake in cultured adipocytes (24). To confirm these data, fully differentiated 3T3-L1 adipocytes were pretreated with various concentrations of GH for 24 h and subsequently subjected to an acute (15 min) stimulation with 0.1 nM insulin. In the absence of GH pretreatment, insulin stimulation resulted in a robust increase in glucose uptake (Fig. 1*A*). However, pretreatment with GH inhibited insulin-stimulated glucose uptake in a GH concentration-dependent manner. As expected, insulin-stimulated glucose uptake occurred in an insulin concentration-dependent manner in the absence of GH pretreatment (Fig. 1*B*). GH inhibited insulin-stimulated glucose uptake at low insulin concentrations, but at higher concentrations (10–100 nM insulin) the full extent of glucose uptake was achieved. These data demonstrate that GH pretreatment results in an insulin-dependent decrease in sensitivity (concentration) but not responsiveness (maximum effect).

We next examined the time dependence of GH pretreatment on insulin-stimulated glucose uptake (Fig. 1*C*). GH pretreatment for up to 48 h had no significant effect on basal glucose uptake. However, after 18 h of GH pretreatment, the extent of insulin-stimulated glucose uptake was significantly reduced. The GH reduction of insulin-stimulated glucose uptake continued to decrease with longer GH pretreatment, and by 48 h glucose uptake was completely refractory to insulin stimulation. In comparison, the effect of GH was also slowly reversible in that following 24 h of GH pretreatment, wash out of GH resulted in a time-dependent recovery of insulin-stimulated glucose uptake (Fig. 1*D*). Taken together, these data demonstrate that GH pretreatment of 3T3-L1 adipocytes results in a reversible,

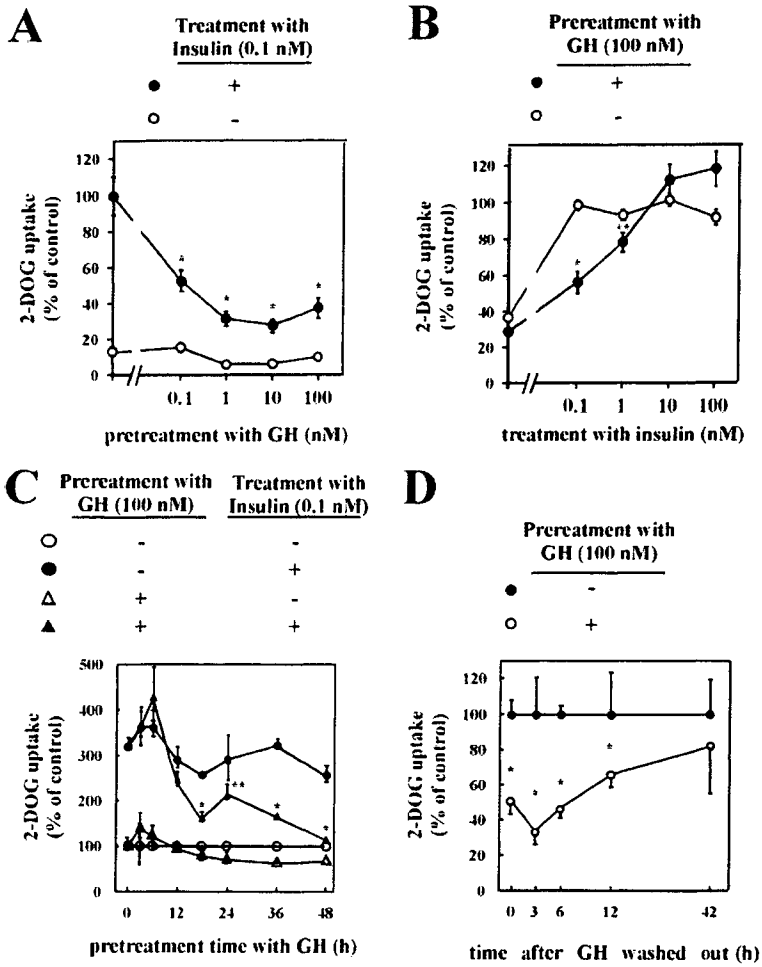

FIGURE 1. **Effects of chronic GH pretreatment on insulin-induced glucose uptake.** *A*, 3T3-L1 adipocytes were serum-starved for 2 h, pretreated with the indicated concentrations of GH for 24 h, and then stimulated without (○) or with (●) 0.1 nM insulin for 15 min. Cells were assayed for glucose uptake as described under "Experimental Procedures." Glucose uptake by cells without GH pretreatment and with insulin stimulation was used as control. *B*, 3T3-L1 adipocytes were serum-starved for 2 h, pretreated without (○) or with (●) 100 nM GH for 24 h, and then treated with the indicated concentrations of insulin for 15 min. Cells were assayed for glucose uptake as described under "Experimental Procedures." Glucose uptake by cells without GH pretreatment and with 0.1 nM insulin stimulation was used as control. *C*, 3T3-L1 adipocytes were pretreated without (●, ○) or with (▲, △) 100 nM GH for indicated periods, and then treated without (○, △) or with (●, ▲) 0.1 nM insulin for 15 min. Next, cells were assayed for glucose uptake as described under "Experimental Procedures." Glucose uptake by cells without GH treatment and without insulin stimulation was used as control. The results are presented as the means ± S.E. of five wells. The difference between insulin-stimulated cells with and without GH pretreatment is significant with $p < 0.01$ (*) or $p < 0.05$ (**). *D*, cells were pretreated with 100 nM GH for 24 h, and GH was washed out by changing medium without GH, followed by incubation for the indicated time. Cells were treated with 0.1 nM insulin for 15 min, and glucose uptake was measured. Glucose uptake by cells without GH pretreatment was used as control. The results are presented as the means ± S.E. of five wells. The difference between cells with and without insulin stimulation is significant with $p < 0.05$ (*). *2-DOG*, 2-deoxy-D-glucose.

time-, and concentration-dependent inhibition of insulin-stimulated glucose uptake.

Chronic GH Pretreatment Does Not Affect Insulin-stimulated GLUT4 Translocation to Plasma Membrane—Two facilitative glucose transporters are expressed in 3T3-L1 adipocytes with the GLUT1 isoform primarily contributing to basal glucose uptake and GLUT4 to insulin-stimulated glucose uptake (2, 34). The cellular expression levels of GLUT1 and GLUT4 were unaffected by chronic GH treatment (Fig. 2*A*). Insulin stimulation increases glucose uptake by the translocation of the GLUT4 isoform from intracellular storage sites to the plasma membrane (35). As expected, biochemical isolation of a plasma membrane-enriched fraction demonstrated the increased appearance of the GLUT4 protein following insulin stimulation (Fig. 2*B*, *1st* and *2nd lanes*). Surprisingly however, chronic GH pretreatment had no significant effect on the extent of insulin-stimulated GLUT4 appearance in the plasma membrane fraction (Fig. 2*B*, *3rd* and *4th lanes*).

To determine whether GH pretreatment altered the fusion (exofacial exposure) of the GLUT4 protein with the plasma membrane, intact adipocytes were incubated with NHS-LC biotin to label plasma membrane proteins with biotin. Precipitation of cell lysates with streptavidin-agarose beads demonstrated an insulin-stimulated increase in the amount of exofacial labeled GLUT4 (Fig. 2*C*, *1st* and *2nd lanes*). Similar to the translocation assay, insulin was fully capable of inducing the plasma membrane fusion (exofacial exposure) of GLUT4 in cells chronically pretreated with GH (Fig. 2*C*, *3rd* and *4th lanes*). As controls, there was a reciprocal decrease in the amount of GLUT4 presence in the supernatant following streptavidin-agarose precipitation (Fig. 2*C*, *bottom panel*). Moreover, there was no precipitation of the GLUT4 protein by streptavidin-agarose beads without NHS-LC biotin labeling (Fig. 2*C*, *5th* to *8th lanes*). These data from three experiments are quantified in Fig. 2*C*, *bar graphs* of the *lower panel*. To morphologically confirm these biochemical findings, we next expressed the GLUT4 protein harboring an exofacial Myc epitope tag. 3T3-L1 adipocytes were electroporated with myc-GLUT4-GFP-expressing plasmids, and the cell exofacial exposure of the Myc epitope was determined following various treatments by confocal fluorescent microscopy (Fig. 2*D*). Insulin stimulation increased the amount of the exofacial exposure of the Myc epitope, and this was again unaffected by chronic GH pretreatment.

The inhibition of insulin-stimulated glucose uptake by GH pretreatment with normal GLUT4 translocation and plasma membrane fusion could have arisen from a reduction in hexokinase activity that phosphorylates 2-deoxyglucose to generate the product 2-deoxyglucose 6-phosphate. To exclude this

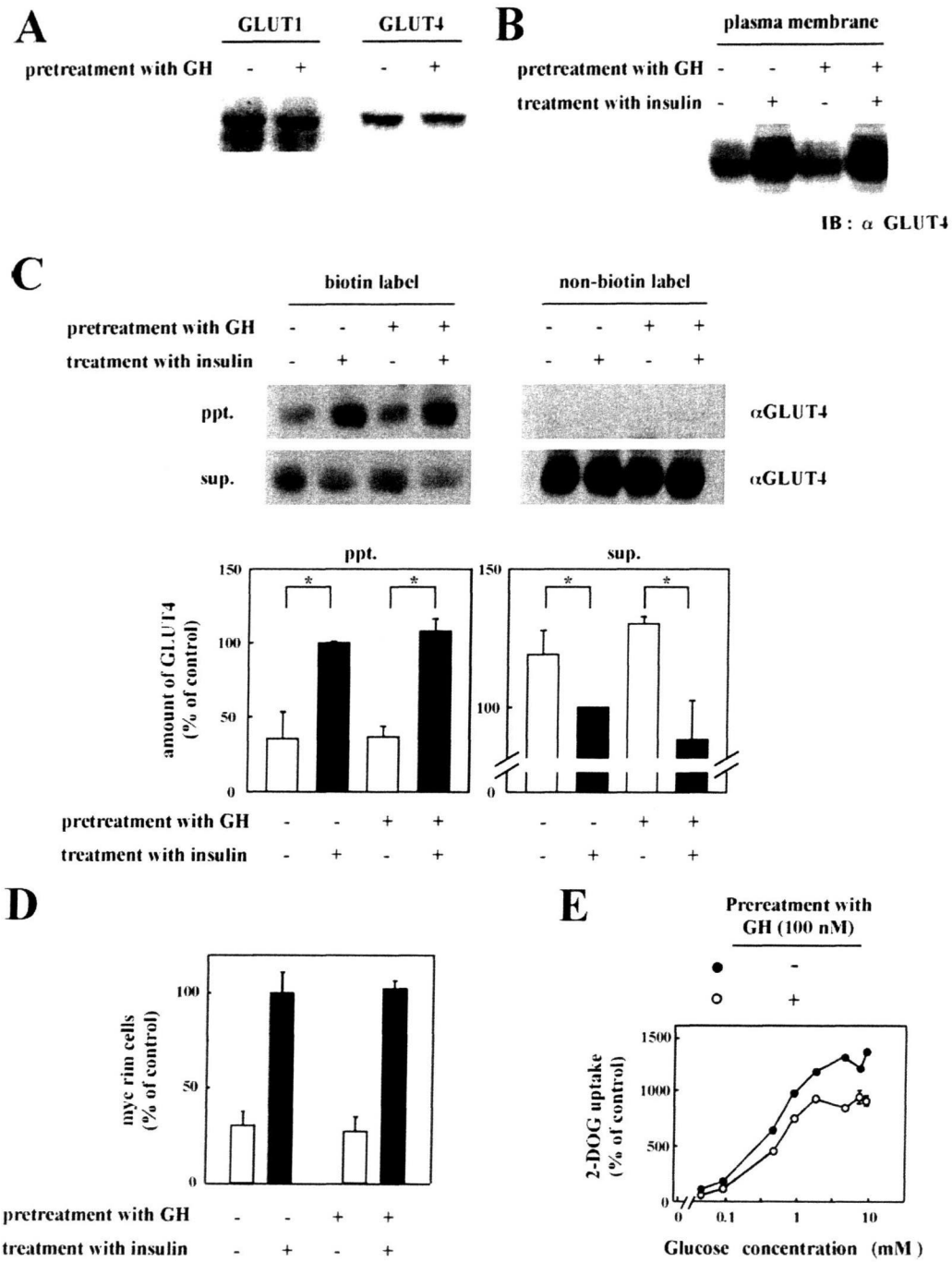

FIGURE 2. **Effects of chronic GH pretreatment on insulin-induced translocation of GLUT4 to plasma membrane.** *A*, 3T3-L1 adipocytes pretreated with or without 100 nM GH for 24 h were lysed by lysis buffer. Lysates were carried out for immunoblotting with anti-GLUT1 antibody or anti-GLUT4 antibody. *B*, 3T3-L1 adipocytes were pretreated with or without 100 nM GH for 24 h and then treated with or without 0.1 nM insulin for 20 min. Subcellular fractions were prepared as described under "Experimental Procedures." Proteins in plasma membrane fraction were separated by SDS-PAGE and immunoblotted (*IB*) with anti-GLUT4 antibody. *C*, 3T3-L1 adipocytes pretreated with or without 100 nM GH followed by treatment with 0.1 nM insulin were biotinylated by incubating with NHS-LC biotin. For isolating biotinylated protein, whole cell lysates were incubated with streptavidin-agarose beads. The pellet (*ppt*) as biotinylated protein and supernatant (*sup.*) as nonbiotinylated protein were collected. Biotinylated proteins and nonbiotinylated proteins were separated by SDS-PAGE and immunoblotted with anti-GLUT4 antibody. Under the blotting images, the quantitative data are shown. The results are presented as the means ± S.E. of three independent experiments. The difference between cells with and without insulin stimulation is significant with $p < 0.05$ (*). *D*, 3T3-L1 adipocytes were electroporated with pGLUT4-myc-GFP as described under "Experimental Procedures." Electroporated cells pretreated with or without 100 nM GH for 24 h were treated with or without 0.1 nM insulin for 15 min. Cells were then fixed without permeabilization and immunostained with anti-Myc antibody to detect cells with GLUT4 fused to plasma membrane. Average of percentage of cells showing GLUT4-myc-GFP rim on the cell surface was calculated. The ratio of GLUT4-myc on the cell surface in insulin-stimulated cells without GH pretreatment was used as control. *E*, 3T3-L1 adipocytes pretreated with or without 100 nM GH for 24 h were treated with 0.1 nM insulin for 15 min. Then various concentrations (0.045, 0.091, 0.45, 0.91, 1.82, 4.5, 7.28, and 9.1 mM) of 2-deoxy-D-glucose (*2-DOG*) containing 10 mCi/ml 2-deoxy-D-[2,6-^{3}H]glucose were added, and radioactivity taken up by the cells was measured. Glucose uptake by the cells with insulin stimulation without GH pretreatment and treated with 0.045 mM 2-deoxyglucose was used as control.